INVESTIGATION OF DISPERSION, STABILITY, AND TRIBOLOGICAL PERFORMANCE OF OIL-BASED ALUMINUM OXIDE NANOFLUIDS

THESIS FOR THE DEGREE OF
MASTER OF SCIENCE IN MECHANICAL ENGINEERING

STEVEN J. THRUSH

OAKLAND UNIVERSITY

2012

Report Documentation Page

Form Approved
OMB No. 0704-0188

1. REPORT DATE	2. REPORT TYPE	3. DATES COVERED
16 NOV 2012	**Master's Thesis**	**06-05-2012 to 01-11-2012**

4. TITLE AND SUBTITLE	5a. CONTRACT NUMBER
INVESTIGATION OF DISPERSION, STABILITY, AND TRIBOLOGICAL PERFORMANCE OF OIL-BASED ALUMINUM OXIDE NANOFLUIDS	**W56H2V-08-C-0236**
	5b. GRANT NUMBER
	5c. PROGRAM ELEMENT NUMBER
6. AUTHOR(S) **STEVEN THRUSH**	5d. PROJECT NUMBER
	5e. TASK NUMBER
	5f. WORK UNIT NUMBER
7. PERFORMING ORGANIZATION NAME(S) AND ADDRESS(ES) **Oakland University,2200 N. Squirrel Road,Rochester,Mi,48309**	8. PERFORMING ORGANIZATION REPORT NUMBER **; #23501**
9. SPONSORING/MONITORING AGENCY NAME(S) AND ADDRESS(ES) **U.S. Army TARDEC, 6501 East Eleven Mile Rd, Warren, Mi, 48397-5000**	10. SPONSOR/MONITOR'S ACRONYM(S) **TARDEC**
	11. SPONSOR/MONITOR'S REPORT NUMBER(S) **#23501**

12. DISTRIBUTION/AVAILABILITY STATEMENT
Approved for public release; distribution unlimited

13. SUPPLEMENTARY NOTES

14. ABSTRACT

The term nanofluid was first proposed by Choi in 1995 and has been studied ever since due to their unique characteristics. Despite their great promise for thermal and tribological properties, the issue of preparing stable and well-dispersed solutions has been the major problem with this new classification of fluid. In this study, the effects of different dispersion procedures and methods on the stability of oil-based Al2O3 nanofluids were investigated. Sample concentration of surfactant and nanoparticles was studied for solution stability. Sample stability was also compared using a different stabilizing agent. The experimentally determined tribological performance for stabilized alumina nanofluids was investigated. Ball-on-disk tests were conducted and friction data was collected over time. The resulting wear data was analyzed using an optical surface profiler. The stabilized nanofluid was tested for enhanced thermal properties. A semi-transient hot plane method was used to acquire thermal conductivity data.

15. SUBJECT TERMS

16. SECURITY CLASSIFICATION OF:			17. LIMITATION OF ABSTRACT	18. NUMBER OF PAGES	19a. NAME OF RESPONSIBLE PERSON
a. REPORT **unclassified**	b. ABSTRACT **unclassified**	c. THIS PAGE **unclassified**	**Public Release**	**85**	

INVESTIGATION OF DISPERSION, STABILITY, AND TRIBOLOGICAL PERFORMANCE OF OIL-BASED ALUMINUM OXIDE NANOFLUIDS

by

STEVEN J. THRUSH

A thesis submitted in partial fulfillment of the
requirements for the degree of

THESIS FOR THE DEGREE OF
MASTER OF SCIENCE IN MECHANICAL ENGINEERING

2012

Oakland University
Rochester, Michigan

APPROVED BY:

Qian Zou, Ph.D., Chair	Date
James David Schall, Ph.D.	Date
Gary C. Barber, Ph.D.	Date

To my mother and father,

Debra and Christopher Thrush.

ACKNOWLEDGMENTS

I would like to thank my advisor, Professor Qian Zou for her continual supervision and mentorship over my graduate career. Her passion inspired me to not only make Tribology my Masters work, but to also pursue a career in Tribology.

I would like to express my gratitude towards my committee members, Professor J. David Schall and Professor Gary Barber, for providing integral guidance in developing the direction of my thesis.

I would like to thank my academic peers. Their camaraderie and mutual guidance helped me strive for excellence.

This thesis would not have been possible without the continual support and encouragement from my family.

I would like to thank the U.S. Army TACOM Life Cycle Command for funding my research under contract number W56H2V-08-C-0236, through a subcontract with Mississippi State University.

Steven J. Thrush

ABSTRACT

INVESTIGATION OF DISPERSION, STABILITY, AND TRIBOLOGICAL PERFORMANCE OF OIL-BASED ALUMINUM OXIDE NANOFLUIDS

by

Steven J. Thrush

Adviser: Qian Zou, Ph.D.

The term nanofluid was first proposed by Choi in 1995 and has been studied ever since due to their unique characteristics. Despite their great promise for thermal and tribological properties, the issue of preparing stable and well-dispersed solutions has been the major problem with this new classification of fluid.

In this study, the effects of different dispersion procedures and methods on the stability of oil-based Al_2O_3 nanofluids were investigated. Sample concentration of surfactant and nanoparticles was studied for solution stability. Sample stability was also compared using a different stabilizing agent. The experimentally determined tribological performance for stabilized alumina nanofluids was investigated. Ball-on-disk tests were conducted and friction data was collected over time. The resulting wear data was analyzed using an optical surface profiler. The stabilized nanofluid was tested for enhanced thermal properties. A semi-transient hot plane method was used to acquire thermal conductivity data.

TABLE OF CONTENTS

TABLE OF CONTENTS—Continued

TABLE OF CONTENTS—Continued

LIST OF TABLES

LIST OF FIGURES

LIST OF FIGURES—Continued

LIST OF ABBREVIATIONS

%vol	Percent concentration by volume (Unit)
%wt	Percent concentration by weight (Unit)
AFM	Atomic Force Microscope
Al_2O_3	Aluminum Oxide
cm^2	Square Centimeters (Unit)
HRB	Rockwell hardness scale B (Unit)
HRC	Rockwell hardness scale C (Unit)
kHz	Kilohertz (Unit)
kJ/mL	Kilojoules per milliliter (Unit)
N	Newton (Unit)
nm	Nanometer (Unit)
PIBSA	Polyisobutylene succinic anhydride
Ra	Root mean squared surface roughness (Unit)
XPS	X-ray photoelectron microscopy

CHAPTER ONE

INTRODUCTION

1.1 Motivation

Ever since Choi composed the term nanofluid [1] research has been expanding to explore the full potential of this new fluid classification. The term nanoparticle refers to a particle with at least one dimension that is within 1-100 nanometers. Nanoparticles can have superior material properties to their bulk material and base fluids counterparts. Therefore, the addition of nanoparticles to a fluid could vastly improve the composite fluid properties of the formulated nanofluid.

Stability of nanoparticles in solution can be a major problem depending on the nanofluid system. Agglomeration can arise in insufficiently stable nanofluids when the repulsive forces between nanoparticles are not enough to prevent collisions between particles due to random Brownian motion. Agglomeration can lead to the testing of a much larger particle size than intended, leading to inaccurate and non-reproducible data. However, flocculation can be prevented by implementing different surfactants, surface modifications, and dispersion techniques.

Many dispersing techniques have been implemented for nanofluids over recent years. A few mechanical methods for dispersing nanofluids include stirring, shaking, and ball milling. An ultrasonic approach has been used via an ultrasonic homogenizer and an ultrasonic bath. Ultrasonic assisted grinding is a common hybrid between the mechanical

and ultrasonic techniques. Choosing an effective dispersion technique is essential to break agglomerates that occur in nanofluids over time. A uniformly dispersed and stable nanofluid can help increase the accuracy and repeatability of experimental data.

One major area of interest when studying nanofluid performance is the thermal properties of the fluid. Creating a fluid with superior thermal management capabilities could lead to smaller coolant systems requiring less fluid and a smaller fluid pump. Recent research has indicated that a small nanoparticle concentration can lead to a large enhancement in thermal conductivity and diffusivity [2]. However, the enhancement of thermal properties was also accompanied by a large spread in experimental data that current theoretical models cannot successfully predict [3].

Another large area in nanofluid research has been in lubricants. Nanoparticles have been theorized to enhance lubricity by four primary mechanisms: rolling, protecting, mending and polishing [4]. Nanoparticles can act as small bearings that roll between two surfaces in the rolling mechanism. This rolling effect reduces wear and friction due to less surface contact and less sliding friction. The protective film mechanism allows for the wear to occur on the nanoparticle coating instead of the underlying surfaces. This may affect friction depending on the application, but the primary role of this mechanism is a wear reducer. The mending effect states that nanoparticles will move along the surface until a sharp surface geometry change occurs, such as a crack or wear track. The particles will remain in these areas and act as a repaired surface. The polishing effect states that the abrasiveness of the nanoparticles rolling on the surface will grind off nanoscale asperities on the surfaces of the contacting bodies. The resulting surface is flatter, making the real area of contact closer to the apparent area of contact [4].

1.2 Research Objectives

The objective of this research is to investigate the stability, dispersion, thermal properties and tribological performance of alumina nanofluids. AFM images will be conducted to determine the state of dry nanopowder. The stability of nanofluids are evaluated using two different stabilizing agents and by comparing sedimentation layers and supernatant sizes over time. Two different dispersion devises will be used, i.e. ultrasonic homogenizer and ultrasonic bath. The order in which nanofluids are prepared will be scrutinized to ensure an optimal preparation method. Thermal conductivity is experimentally collected for a stable alumina nanofluid. The tribological performance of alumina nanofluids are determined by analyzing friction and wear.

1.2.1 Nanofluid Stability

The stability of alumina nanofluids is studied. Pure mineral oil is selected as a control to ensure the effects of the stabilizing agents are not affected by additives. Multiple concentrations of one surfactant will be tested to seek out an optimally stable ratio between nanoparticles and surfactant. The stabilizing ability of two different surfactants is compared by monitoring the formation of the supernatant and sedimentation layer for each nanofluid.

1.2.2 Nanofluid Dispersion

A Branson 1510 Ultrasonic Bath and Omni Sonic Ruptor 400 Ultrasonic Homogenizer are used in the dispersion study. This is done by analyzing particle size distributions using a Malvern Zetasizer NS before and after ultrasonic energy is applied to alumina nanofluids. Different durations of ultrasonic power are applied to alumina

nanofluids to investigate how much energy is required to achieve an optimum dispersion with each method. The Malvern Zetasizer NS is also used to investigate the order to mix and disperse a nanofluid.

1.2.3 Thermal Properties

Thermal conductivity is analyzed using a C-Therm Technologies TCi Thermal Conductivity Analyzer. A stabilized nanofluid is compared against oil, oil with particles, and oil with stabilizing agent.

1.2.4 Tribological Performance

Tribological performance is analyzed for stabilized alumina nanofluids at two different concentrations of alumina nanopowder. First, ball-on-disk tests are conducted using a Universal Micro-Tribometer (UMT-3). Friction over time data is automatically collected by the tribometer. The wear track on the steel disk and wear scar on the ball are analyzed for wear area and wear volume using a Bruker NPFLEX. The wear track generated using an alumina nanofluid is also investigated using a scanning electron microscope. A ceramic ball is used in the same test configuration to help maintain the contact pressure generated by the applied load for the duration of the tests.

CHAPTER TWO

LITERATURE REVIEW

Nanofluid technology has been a rapidly growing field since its conception was proposed by Choi almost two-decades ago. The main areas of research are in coolant and lubricant enhancement. Scientists have been researching nanofluids for thermal properties, load capacity, friction and wear performance, and corrosion resistance. In most cases, the unique material properties of nanoparticles are reflected in an enhancement of the bulk fluid properties. The performance of nanofluids, however, is dependent on the stability and dispersibility of the nanoparticles. Agglomerated nanoclusters can induce intrinsic error when experimentally investigating nanofluids, thus their effect must be minimized.

2.1 Stability of Nanofluids

The main obstacle affiliated with nanofluids is maintaining stable solutions. Research has been done to modify nanoparticle surfaces through esters, ligands, and other hydrophobic/hydrophilic materials. Nanoparticles can also be stabilized in solution with the use of a surfactant. Surfactants vary from fatty acids, commercial products, or custom synthesized molecules. The effectiveness of the stabilizer is specific to the nanofluid system. An appropriate stabilizing technique increases the repulsive steric force between particles. These steric forces must be sufficient to overcome short-range van der Waals attractive forces to help reduce collisions brought on by Brownian motion.

If the net force is not sufficiently strong, the randomly moving particles collide with each other and agglomerate. This could ultimately lead to invalid experimental results due to improper stabilization and nanoparticle characterization when testing highly flocculated nanofluids.

Stiller et al., [5] used solid alumina particles to surface treat titanium oxide nanoparticles in both water-in-oil and oil-in-water emulsions. The titanium oxide nanoparticles were reported to have an average diameter of 7-9 nm and a length of 60 nm. They found that the coating altered the hydrophobicity of the particles. The alumina coating was also treated with an increasing amount of a hydrophobic agent called simethicone. With increasing concentration of this additive, the contact angle of water increased. The contact angle data directly predicted the stabilization properties of the titanium oxide nanoparticles. They concluded that the stability of the surface treated nanoparticles in a water-in-oil emulsion increased with increasing contact angle. However, increasing contact angle decreased the stability of an oil-in-water emulsion.

Using ligands as a surface coating for nanoparticles was investigated by Mulvihill et al., [6]. They preformed a two-phase interfacial exchange method using cadmium selenide nanoparticles to produce a stable aqueous nanofluid. This method was used to investigate the effect of ligand chain length on particle stability. They found that nanoparticles coated with long chained ligands (eleven carbons) showed superior stability than the shorter chained ligands tested. Available surface area for coating and ligand length were concluded to be the major factors in stabilizing cadmium selenide nanoparticles.

Surface stabilizing nanopowder as a precursor to redispersion was investigated by Simakov and Tsur [7]. They used titanium dioxide nanoparticles in a hydrolysis-precipitation method to surface treat the nanoparticles with diethylene glycol monomethyl ether. When the surface treated nanoparticles were dried and redispersed in aqueous solution, they showed superior stability over the untreated nanoparticles. They concluded that the surface treatment prevented direct contact between nanoparticles when the nanoparticles precipitated and dried. This resulted in a more porous nanopowder with weaker bonds between individual particles. The resulting nanopowder was more easily deagglomerated using an ultrasonic homogenizer when redispersed in an aqueous solution.

Kole and Dey [8] investigated the stability and viscosity of in a commercially available automotive coolant with the addition of alumina nanoparticles. They used alumina nanoparticles of a nominal diameter less than 50 nm and suspended it in 50% polyethylene glycol and 50% water solution. Oleic acid was used as a stabilizing agent. They concluded that with a controlled amount of oleic acid and sufficient dispersion, they could maintain a stable alumina nanofluid solution for 80 days. Their definition of a stable nanofluid was no sedimentation or supernatant formation for the full time duration. However, the nanocoolant formulation that was stable exhibited non-Newtonian fluid behavior. This could allude to the force generated from the viscosity tests deagglomerating nanoclusters or the disintegration of surfactant-nanoparticle networks.

Bell et al., [9] used fatty acids to stabilize alumina nanoparticles in decalin. The alumina nanoparticles had an average diameter of 50 nanometers, but were reported to have particles ranging from 10 to 400 nanometers. The fatty acids chosen were

propionic, valeric, heptonic, and oleic acid. The resulting stability test showed that oleic acid had the best performance as a stable supernatant. However, the agglomeration and sedimentation process was evident for this nanofluid. Oleic acid was the longest hydrocarbon chain length of the fatty acids chosen and it was estimated to have the longest steric length of 2.5 nm. Having the longest steric length increased the steric repulsion force, which could have been the dominant factor contributing to its superior ability to stabilize nanofluids.

Li et al., [10] studied several different surfactants and their effect on an aqueous copper nanofluid. They used a non-ionic surfactant in polyoxyethylene nonyl phenyl ether, a cationic surfactant called hexadecyl trimethyl ammonium bromide, and an anionic surfactant called sodium dodecylbenzenesulfonate. These surfactants were chosen due to their widely different effect on charging of surfaces. One study they performed was on a solution containing 0.1g copper nanoparticles, 0.1g of cationic surfactant, and 99.8g of water solution dispersed using an ultrasonic vibrator for one hour at 100 watts and 40 kHz. They found a dramatic difference between the presence and absence of surfactant that was 130 nm and 5560 nm average particle size respectively. The solution with surfactant was also stable for one week without any sedimentation. They found that optimum dispersion using the three different surfactants was achieved with 0.43%wt for the non-ionic, 0.05%wt for the cationic, and 0.07%wt for the anionic surfactant. Thus, the ionic surfactants could produce stable solutions at much lower concentrations.

Somasundaran and Huang [11] discussed the potential synergistic effects of mixing surfactants on metal surfaces. When surfactants are mixed together, they compete

and produce a dynamic effect on coating surfaces and forming critical micelle concentrations. This competition when applied to nanotechnology could improve nanofluid stability. Having two surfactants of widely varying chain lengths could potentially improve the surfactant density of a coated surface and increase the steric repulsion force.

Unique surfactants can be synthesized and used as stabilizing agents in nanofluids. Amstad et al., [12] investigated surface functionalizing iron oxide nanoparticles for magnetic resonance imaging application. They created a custom surfactant by using a polyethylene glycol hydrocarbon and gallol molecule. This research resulted in improved particle stability due to the high affinity between the surfactant and nanoparticles.

Chemat et al., [13] analyzed how ultrasonic homogenization affected the oxidation of sunflower oil. Sunflower oil is composed of several different fatty acids, and, as seen previously, fatty acids can be used as stabilizing agents in nanofluids. They concluded that with ultrasonic treatment of 150 watts at 20 kHz for 0.2 to 2 minutes, some degradation and oxidation of the fatty acids contained within sunflower oil was observed. With this in mind, deteriorated oleic acid when used as a stabilizing agent in nanofluids could alter the expected stabilizing performance.

2.2 Dispersion of Nanofluids

Several dispersion methods have been implemented in nanofluid applications: including magnetic stirring, mechanical stirring, ultrasonic bath, ultrasonic homogenizer, high-pressure homogenization, ball mill grinding, and ultrasonic-assisted grinding to

name a few. The ultrasonic techniques have grown in popularity due to their ease of implementation, effectiveness as a dispersing tool, and low cost. A proper dispersion technique has to be investigated for all nanofluid studies to characterize nanofluid agglomerate concentration. Dispersion time, energy, etc needed to break agglomerates and reach an optimum dispersion must be determined. If proper nanofluid characterization is not achieved with a dispersion test, there is a risk of experimentally testing an inferior and uncharacteristic agglomerated nanofluid.

Ding and Pacek [14] researched dispersing hematite nanopowder in the presence of a surfactant. They used an ultrasonic processor as a dispersing tool. First, a dry hematite powder was wetted in an aqueous solution and sodium polyacrylate was used as the stabilizing agent. The solution was then ultrasonicated and the energy input was calculated via a calorimetry method using the heat generated from the ultrasonication process. The processed nanofluids were characterized for particle size distribution and zeta potential. The concentration of hematite, concentration of stabilizer, pH and energy input were all varied to understand the dispersion and stability of aqueous hematite nanofluids. The results indicated there was an optimum concentration of surfactant needed to stabilize the nanofluid. Additional stabilizer would promote agglomeration via surfactant networking. Altering pH had a great effect on the zeta potential of the sample and the deagglomeration of nanoclusters. They concluded that deagglomeration was only possible in the presence of a surfactant while altering pH also helped the ultrasonic dispersion process.

Xiong et al., [15] dispersed titanium carbide nanoparticles in water using Tween 80 as a surfactant. The titanium carbide nanoparticles had an average particle diameter of

40 nm. They dispersed the titanium carbide nanoparticles using an ultrasonic homogenizer at 100 watts and 40 kHz for varying time durations. Under these conditions, they found that the ultrasonic process showed diminishing returns with respect to average particle size after 30 minutes. They also studied the effect of surfactant concentration on nanofluid sedimentation. The sedimentation volume was minimized when adding 0.5%V Tween 80 to stabilize 0.1%V of titanium carbide nanoparticles. Lower surfactant concentrations were not able to stabilize the nanofluids, and higher concentrations promoted agglomeration because the excess surfactant formed large networks. A similar study was conducted by Bihari et al., [16] that also investigated the process by which to mix and disperse nanofluids using titanium oxide, water, and Tween 80. Again, there was an optimum dispersion achieved through ultrasonication, where additional energy applied to the nanofluid did not further reduce the average nanoparticle size. They found that the optimal mixing procedure was to first add the dry titanium oxide powder to water, then apply ultrasonic power to deagglomerate the nanoparticles, next to add stabilizing agents, and finally add a salt solution.

Hwang et al., [17] studied the dispersion of carbon black nanoparticles suspended in water and silver nanoparticles suspended in silicon oil. The aqueous carbon black nanofluid had a 1%wt concentration of sodium dodecyl sulfate to help promote stability. The silver oil-based nanofluid contained 1%wt of oleic acid for the same purpose. They dispersed the nanofluids using five different techniques: no physical treatment, stirrer, ultrasonic bath, ultrasonic disruptor, and a high-pressure homogenizer. Dispersion was conducted until diminishing returns were reached. Analyses were accomplished by

taking particle size distributions after the dispersion process was completed. For no physical treatment, the authors simply suspended the nanoparticles in the base fluid, but did not apply any energy to disperse them. The stirrer method used only mechanical stirring and had limited effect on breaking agglomerated particles. Ultrasonic bath refers to a method in which the test vial is placed in a water bath and ultrasonic energy is applied to the water, which then travels through the test vial, finally reaching the nanofluid. This technique is superior to solely using a stirrer but still does not effectively disintegrate the particles. They found that ultrasonic disruption was quite effective in dispersing nanoparticles. Ultrasonic energy was directly applied to the lubricant via a titanium processing tip that resonates at high frequency. This method achieved the best dispersability that was also cost effective. High-pressure homogenization requires a more expensive experimental setup as well as more power for negligible difference in particle size distribution data when compared to the ultrasonic disruption technique. They concluded that in order to get stable, well-dispersed nanofluid solutions, a high energy deflocculating process must take place in the presence of a stabilizing agent.

Roebben et al., [18] conducted a multi-laboratory round-robin study to investigate the reproducibility of nanofluid characterization. All laboratories used strictly, quality controlled nanofluids in the NIST RM 8012 and IRMM-304. The NIST RM 8012 nanofluid is an aqueous solution that contains 30 nm citrate-stabilized gold nanoparticles. The IRMM-304 is a 40 nm diameter silica nanofluid with sodium hydroxide as a stabilizer. There was some variability between laboratories in both particle size distribution and zeta potential. They concluded that the sonication process prior to data acquisition needed to be controlled more thoroughly, citing it as the major factor for the

variability in data. They also noted that this test had inconsistencies using stable, quality controlled nanofluids. A study with unstable or polydispersed nanofluids could prove to be even more problematic.

2.3 Thermal Conductivity of Nanofluids

A wide range in nanofluid thermal conductivity results have been published over recent years. Primarily, research in nanofluid thermal conductivity has pertained to water or water/ethylene glycol mixtures due to their practical applications for coolants. Nanoparticle types tested range from metal oxides, pure metals, nanotubes, and lamellar structured nanoparticles including platelets and fullerenes. Most trends of nanoparticle concentration versus thermal conductivity follow a linear trend as current theoretical models also predict. However, some anomalous thermal conductivity data have been reported, particularly at very low nanoparticle concentrations (<1%wt). The irregular results sparked great controversy and intrigue.

2.3.1 Metal Oxide Nanoparticles

Zhu et al., [19] investigated aqueous alumina nanofluids for a dispersion and thermal conductivity study. First, the pH of the nanofluid was altered to find a stable solution. They quantified stability by analyzing the zeta potential of the solutions throughout the full pH range (0-14). A stable alumina nanofluid was found at a pH between 8 and 9. The stable solution was then used for thermal conductivity measurements at different alumina concentrations using a transient plane source. With just 0.15%wt alumina nanoparticles, the nanofluid exhibited a 10.1% increase in thermal

conductivity. This was the highest enhancement found and also the highest alumina concentration tested.

Zhu et al., [20] created a synthesis method to prepare stable copper oxide nanoparticles in water. The particle size range they achieved was 30-90 nm with an average particle diameter of 50nm. The particles were stabilized with ammonium citrate. The dispersed and stable nanofluids were tested for thermal conductivity. The resulting thermal conductivity enhancements with increasing copper oxide concentration were 18% for 1%vol, 28% for 3%vol, and 31% for 5%vol. This trend was nonlinear, as the increase in thermal conductivity enhancement barely increased when increasing the nanoparticles concentration from 3 to 5% by volume.

2.3.2 Pure Metal Nanoparticles

A comparison study conducted by Xuan and Li [21] prepared similar samples to that of a previous article on thermal conductivity enhancement of nanofluids conducted by Eastman et al., [22]. They prepared a transformer oil nanofluid with copper nanoparticles and oleic acid as the stabilizer. They also prepared an aqueous copper nanofluid using laurate salt as a stabilizer. They used a transient hot wire apparatus and analyzed both nanofluids for thermal conductivity enhancement with increasing nanoparticles concentration. They found a consistently lower performance for both nanofluids when compared to a previous work, but the aqueous solution had closer agreement. The trend was linear and had a similar slope as Eastman. They hypothesized that the large difference in the oil nanofluid results was potentially due to the size difference of the copper particles that were chosen for the study.

2.3.3 Dispersion Effect on Thermal Conductivity

Nasiri et al., [23] investigated the change in thermal conductivity enhancement over time with nanofluids. For this study, single, double, and multi-walled carbon nanotubes were used in aqueous solutions. Sodium dodecyl sulfate was used as a stabilizing agent. An ultrasonic bath and ultrasonic homogenizer were investigated in this study to understand if one dispersion method was more resilient to reagglomeration over time. The ultrasonic homogenizer resulted in consistently smaller particle size distributions and larger thermal conductivity enhancements over time. This alludes to the ultrasonic homogenizer being the superior method to disperse nanofluids. It also showed how critical the dispersion step was to collect an accurate experimental measurement. However, both methods observed a decrease in thermal conductivity over time. Thermal conductivity data was collected for 400 hours after ultrasonic energy was applied and both methods showed a similar performance decrease with time duration. The stability of the nanofluid greatly affected the performance for thermal conductivity measurements because if the nanofluids were unstable, severe agglomeration would take place and accurate measurement could be experimentally taken.

2.4 Tribological Performance of Nanofluids

Nanofluids have shown great promise in tribology applications. Much like the nanofluid research regarding thermal property enhancement, a variety of different nanoparticle types were investigated over recent years. Metal oxides, pure metals, lamellar structures, and nanotubes have all been examined by research teams in lubrication studies. Particle concentration, size, and shape have primarily been

investigated. Lee et al., [4] discussed four primary mechanisms in an effort to justify the benefit of nanoparticles in lubricants; rolling, mending, polishing, and protecting. The role of each mechanism depends on the lubricating conditions and the type of nanoparticle.

2.4.1 Metal Oxide Nanoparticles

Hernandez Battez et al., [24] explored three different metal oxide nanoparticles in a tribological study. Copper oxide, zinc oxide, and zirconium oxide nanoparticles were individually tested in a block-on-ring configuration. The applied load was 165 N and sliding speed was 2 m/s for a total sliding distance of 3 meters. The particles were suspended in polyalphaolefin oil at concentrations ranging from 0.5% to 2%wt. The nanofluid suspensions were dispersed for 2 minutes with an ultrasonic probe prior to testing. Each test was run twice to reduce data noise. All nanofluid samples tested showed a friction reduction. These friction reductions were accompanied by wear reductions except for the 1%wt zirconium oxide nanofluid. The maximum friction reduction exceeding 20% occurred at the lowest particle loading for both zinc oxide and zirconium oxide. The maximum wear reduction for these nanofluids also occurred at the minimum particle loading, showing over a 50% reduction. From this research, the tribological performance of nanofluids was not linearly related to nanoparticle concentration.

Gara and Zou [25], investigated the tribological effects of zinc oxide and aluminum oxide nanoparticles in aqueous solutions. Ball-on-disk tests were performed with a 10 N applied load and a 100 mm/s sliding velocity. A wide range of nanoparticle

concentrations were tested from 0.1 to 50%wt. The stabilizing agent was not disclosed for the commercial aqueous solutions that were purchased. The resulting friction for both types of nanofluid was beneficial across the full range of concentrations tested. However, the collected wear data via an optical method showed a wear reduction only at 0.1%wt zinc oxide and all five different concentrations for alumina nanofluid trials had large wear increases. XPS analysis after the zinc oxide nanofluid trials proved that zinc was present inside the wear track at an atomic concentration of 26.1% and not present outside of the track. In conclusion, the nanofluid tests conducted illustrated a friction reduction provided by a forming of a nanoparticle deposited film layer, but also a large amount of wear.

Gu et al., [26] explored a metal oxide nanoparticle in ceria, but paired it with calcium carbonate. This was done in 40CD oil with a nanoparticle loading of 0.6%wt at a 1:1 ratio by weight between ceria and calcium carbonate. The nanofluids were suspended using four different stabilizing agents at controlled concentrations. The nanofluids were used in a four-ball test for 1 hour with an applied load of 392 N. The steel balls used were GCr15 balls with 12.7 mm diameter. These test conditions yielded a 33.5% reduction in wear scar diameter and a friction reduction of 32% for the nanofluid against the neat oil. XPS analysis illustrated a layer of calcium, cerium and oxides as a protective film that protected the surface. The study was repeated by Gu et al., [27] substituting titanium oxide nanoparticles in the place of calcium carbonate, and 500SN instead of 40CD oil as a base fluid. The ratio between ceria and titania changed to a 1:3 ratio by weight. Under the same test conditions in the four-ball test configuration, they found a 37.7% wear scar diameter reduction and a 37.6% friction reduction.

2.4.2 Pure Metal Nanoparticles

Yu et al., [28] studied the tribological effects of copper nanoparticles in lubricating oil. The copper nanoparticles were surface modified using a ball mill to mix them with a resin acceptor, methylbenzene, and an amine compound for 24 hours. The resulting surface modification made the copper nanoparticles well suited to be dispersed stably into an organic base fluid, such as the 50CC oil chosen for experimentation. The prepared nanofluids contained 0.2%wt 20 nm copper nanoparticles. The nanofluids were tested using a four ball tester with SAE52100 steel, 12.7 mm diameter balls. The test was run at 1200 rotations per minute and a 294 N load for 15 minutes. Tests were run at different temperatures ranging from 25 to 140°C. Each test condition was run three times and averaged to minimize the scattering of data. The performance of the copper nanofluid gradually increased with increasing temperature. At 140°C, there was a wear scar diameter reduction of 25% and a friction reduction of 20%. XPS was performed on the balls after the nanofluid trials were conducted and there was evidence of copper embedded into the surface. The conclusion drawn from this experiment was that the protective copper film of low hardness provided both wear and friction reduction. They also concluded that the higher the localized temperature at the point of contacting bodies, the more likely a soft copper film would occur on the surface.

Wang et al., [29] researched a method to suspend copper nanoparticles in oil for testing with regards to tribological performance. Copper nanoparticles with 20 nm diameter were created by treating the particles with oleic acid, processed with a globe mill, and then dispersed into 650SN oil. The friction wear testing apparatus was operated at 200 rotations per minute with an applied load of 400 N for an hour. The copper

concentrations tested ranged from 0.1% to 1%wt and all solutions tested showed a friction reduction once a steady coefficient of friction was reached. However, the best performing concentrations were at low copper loadings (0.15% and 0.175%wt). They concluded that a reduction of friction at low loadings of copper nanoparticles was possible with a nanofluid of good dispersion and stability characteristics.

2.4.3 Metal Compound Nanoparticles

Different nanoparticle compounds have shown great promise as lubricant additives in literature. Magnesium borate nanoparticles were investigated as a lubricant additive by Hu et al., [30]. Magnesium borate nanoparticles of a 10 nm diameter were dispersed into 500SN oil using sorbitol monostearate as a stabilizing agent. Four-ball tests were run for a nanofluid of 0.757%wt magnesium borate and 1.00%wt sorbitol monostearate in 500SN. The tests were run for 30 minutes with an applied load of 295 N. The wear scar diameter for the nanofluid was 0.43 mm as opposed to a wear scar of 0.69 for the base fluid. Maximum non-seizure load was also found to be 921 N at a 2%wt magnesium borate nanofluid, compared to only 549 N for neat 500SN oil. A block-on-ring test configuration was used to determine the frictional performance of a 0.65%wt magnesium borate nanofluid containing 1.00%wt sorbitol monostearate. This test resulted in a friction reduction throughout the 30 minute trial. The tribofilm generated after the tests were analyzed using an XPS in the contact area. Boron was found, but magnesium was not. Magnesium borate nanoparticles as an oil additive reduced the friction and wear while increasing the load carrying capacity of the fluid. A

protective boron-based film was generated that protected the surface and increased lubricity between the contacting bodies.

Zinc dithiophosphate has been used as a common wear reducing lubricant additive. Zhou et al., [31] formulated a way to functionalize 8 nm copper nanoparticles with dithiophosphate groups to effectively create copper dithiophosphate nanoparticles. These particles were compared for tribological performance against a zinc dithiophosphate counterpart using a four-ball test. The four-ball test was conducted using 4%wt nanofluids and neat oil. The operating conditions were with a rotational speed of 1450 rotations per minute and the ball material was GCr 15 with a 12.7 mm diameter. The tests were conducted to determine the maximum non-seizure load and sintering load. The wear scar diameter was measured with an optical microscope. The copper dithiophosphate nanofluid outperformed zinc dithiophosphate under identical conditions with an increased maximum non-seizure, sintering load, and a reduced wear scar diameter. XPS was performed to understand the chemical morphology of the worn surfaces of the ball and there were copper, sulfur, and phosphate groups present. This protective film was proposed to have better anti-wear capabilities due to its superior performance in experimental testing.

2.4.4 Lamellar Structured Nanoparticles

Lee et al., [4] proposed the mechanisms for nanoparticle friction and wear reduction as part of a carbon fullerene tribological study. A disk-on-disk apparatus was created in an effort to pinpoint the primary mechanisms for improved performance of nanofluids. The test used grey cast iron in an oil bath and the disks were subjected to a

200 to 800 N normal force and a 1,000 rotations per minute speed at 40°C. All fullerene nanofluids were composed of 1%vol, 10 nm carbon fullerenes in mineral oil and were ultrasonicated at 250 watts and 44 kHz for 24 hours. The friction reduction observed at 200 N was roughly 67% and 88% at 800 N when compared to neat mineral oil. However, after the nanofluid trials, the control was repeated and the friction reduction was still present. They concluded that the surface modification and nanoparticle abrasion greatly affected the friction results. The primary mechanism for the friction reduction of the revisited control was not confirmed.

2.4.5 Effect of Dispersion on Tribological Performance

Moshkovith et al., [32] studied the effects of dispersion process as a precursor to tribological testing using 120 nm diameter, inorganic fullerene, tungsten disulfide particles. Tungsten disulfide nanofluids were prepared in paraffin oil at 1%wt and were subjected to ultrasonication. There was delamination of the fullerene particles using this method of dispersion, so they switched to a 75 hour magnetic stir process. A ball-on-flat friction tester was used with a 2 mm steel ball and an AISI 1045 steel flat. The maximum contact pressure was 1 GPa, and the reciprocating velocity was 0.04 mm/s. The mixing time before the friction tests ranged from 1 to 27 hours, and the spread in data was minimized and reproducible data was only possible with a minimum of 15 hours of magnetic stir bar mixing. The friction data converged to a friction range of 0.02 to 0.03 with mixing duration. An AFM was used to determine the mechanism behind the rapid drop in friction with mixing time. Particles were observed to have been embedded into the surface. The longer the mixing time, the more embedded particles were present which

correlated to smaller particles more easily penetrating and mending the surface. The wear track for the nanofluid trials with sufficient mixing also showed untouched steel in the wear track, thus the nanofluids were wear reducing agents as well as friction reducers. This study emphasized the dispersion of nanofluid prior to experimental testing. It is evident that the results can drastically change depending on this critical step of the nanofluid preparation process.

CHAPTER THREE

DISPERSION OF NANOFLUIDS

The purpose of this study is to investigate the agglomeration condition of stock nanopowder and the amount of dispersion energy needed to reach an optimum nanofluid dispersion using two ultrasonic methods. AFM imaging was used to determine the state of the dry powder. Particle size distribution was compared with increasing amount of input energy until diminishing returns were reached for each nanofluid dispersion method.

3.1 Experimental Setup

3.1.1 Test Equipment

An AFM was used to analyze the condition of dry alumina nanopowder because of its ability to achieve nanoscale resolution. AFM imaging can measure surface contours of nonconductive materials, such as ceramics in this case (which is why apparatuses like an STM could not be used without conditioning the sample). The AFM was operated in a noncontact testing mode. In this mode, the AFM is able to detect forces on the order of piconewtons.

The Branson 1510 Ultrasonic Cleaner shown in Figure 3.1 applies a power of 70 watts at 42 kHz to a water bath. The ultrasonic bath is equipped with a timer and heater. This is an indirect method for applying ultrasonic energy because energy is first applied

to the water bath, then the glass vial, and finally to the solution. There is intrinsic energy loss across each of these barriers.

The ultrasonic homogenizer, shown in Figure 3.2, directly applies ultrasonic energy to the nanofluid samples. The applied wattage is variable from 40 to 400 watts in increments of 40 watts at a frequency of 20 kHz. It is equipped with a 0.375 inch titanium processing tip and the maximum power that can be achieved with this particular processing tip is 360 watts. There is a pulse mode option to control sample temperature and disperse nanofluids over a greater amount of time. There is also a timer for precisely timed ultrasonication processes.

The Malvern Zetasizer Nano ZS uses a dynamic light scattering technique to characterize nanofluids with nanometer accuracy. A helium neon laser illuminates the sample at a 173˚ backscatter method. This method was chosen because it increases the accuracy of particle size distribution profiles. It also limits potential error due to multiple scattering and vial reflectiveness. This apparatus is essential to compare nanofluid dispersion methods and the agglomeration state of a nanofluid.

3.1.2 Materials

The dry powder chosen for this investigation was Nanotek alumina nanopowder from Nanophase Technologies with an average particle size of 40-50 nm. It was surface functionalized, but the exact surface chemistry was proprietary information.

Figure 3.1. Branson 1510 Ultrasonic Cleaner Ultrasonicating an Alumina Nanofluid. *(This figure is presented in color; the black and white reproduction may not be an accurate representation.)*

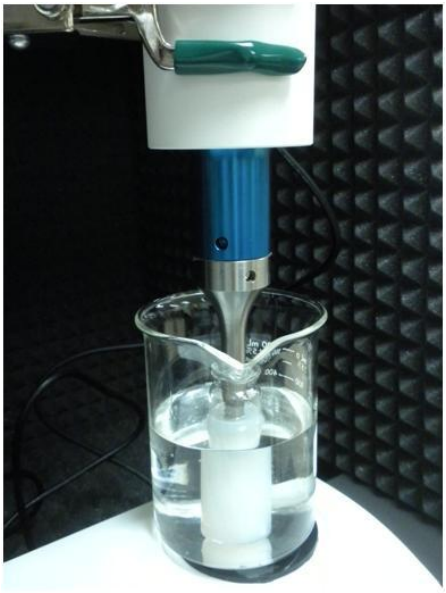

Figure 3.2. Omni Sonic Ruptor 400 Ultrasonic Homogenizer Ultrasonicating an Alumina Nanofluid. *(This figure is presented in color; the black and white reproduction may not be an accurate representation.)*

Choosing base oil suitable for extensive nanofluid research is critical. The oil should have no additives to ensure that the changes in performance are due to the addition of nanoparticles and surfactant alone. A low viscosity mineral oil offers a wide range of low load applications. A light paraffinic oil, Ergon P70N, was chosen as the controlled base fluid of the oil-base nanofluid research because it satisfies the criteria.

The surfactant can greatly affect the stability of the solution. This chemical group is composed of a 'head' and 'tail' component. The hydrophilic heads will orient themselves towards anything that is not oil in an oil system, which means the glass of the test vials, air, and nanoparticles contained in solution. The tail component is a lipophilic hydrocarbon, which has a strong affinity for oil. These orientations equate to an effective charge given to these boundaries. The charges are all similar due to the same surfactant coating of each surface. The length of the hydrocarbon tail directly correlates to the steric length generated by the surfactant coating, thus the steric repulsive force is enhanced using a long-chained surfactant in an oil system. If the steric force is great enough, nanoparticle collisions are kept to a minimum, resulting in a stable nanofluid. Oleic acid (>97% pure) from Fisher Scientific was used due to its 18 carbon long tail.

3.1.3 Sample Preparation

In dry powder evaluation, alumina nanoparticles were wetted, dispersed, and a drop of the aqueous alumina nanofluid was placed on a pre-cleaned glass slide. The slide was placed on a hot-plate until all the water evaporated and dry powder remained. This was done to promote the self-alignment of particles in a more uniform distribution across the glass surface. The slide was then taken to the AFM for analysis.

To investigate the distribution of nanoparticle size in the nanofluids, identical 25 mL samples were prepared using P70N oil containing 0.02%wt alumina nanopowder and 0.28%wt oleic acid. This was accomplished by diluting a 1.0%wt alumina, 14%wt oleic acid nanofluid by a factor of 50. The level of the water bath was controlled equal to the height of the nanofluid in the glass vial as shown in Figure 3.1. The ultrasonic bath was operated at 70 watts for increasing time durations until diminishing returns in particle size distributions were reached. Nanofluids subjected to the ultrasonic homogenizer were also placed in a water bath. The penetration depth of the processing tip into the solution was controlled to be a half inch and was operated at 160 watts, shown in Figure 3.2. A water bath was also used for the ultrasonic homogenizer for heat management. Particle size distribution data was taken immediately after dispersion of each nanofluid sample.

3.2 Results of Dispersion Study

3.2.1 AFM Imaging of Dry Nanopowder

One aspect that was investigated was the condition of the dry nanopowder. AFM is a common method used for a representation due to the required resolution. Figures 3.3 and 3.4 show two and three dimensional representations for the same square micron of dry alumina nanopowder. These figures illustrated that dry alumina powder was highly agglomerated. Some nanoclusters range above 300 nm diameters and most are larger than 150 nm. Agglomerate bonds between the particles effectively created larger particles of several times the average particle size. If these bonds are not broken, it can greatly affect the performance of the nanofluid.

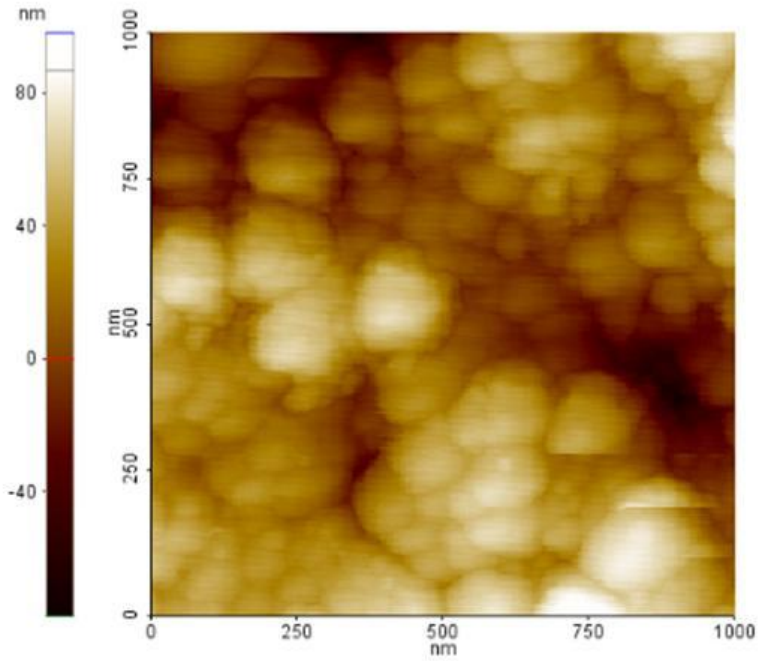

Figure 3.3. 2D AFM Image of Alumina Nanopowder. *(This figure is presented in color; the black and white reproduction may not be an accurate representation.)*

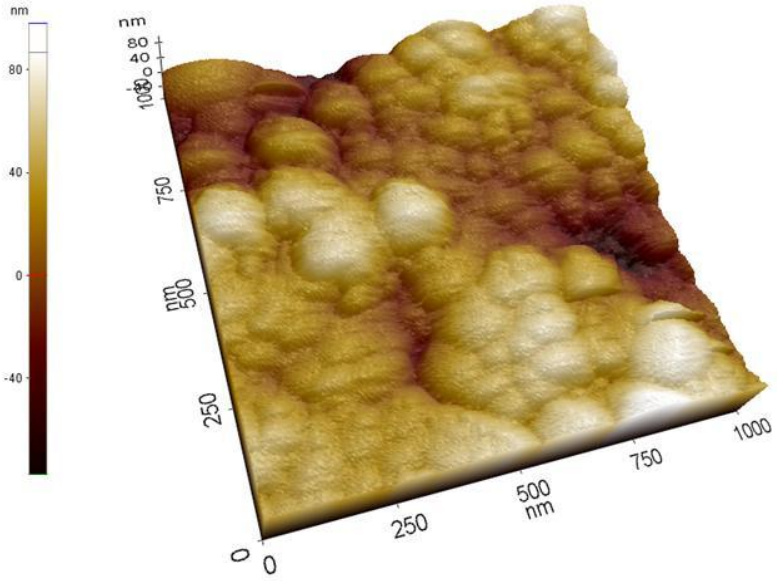

Figure 3.4. 3D AFM Image of Alumina Nanopowder. *(This figure is presented in color; the black and white reproduction may not be an accurate representation.)*

3.2.2 Dispersion of Nanofluids

Ultrasonic methods have been widely used to deagglomerate and disperse nanofluids. This investigation compared the effectiveness of a 70 watt ultrasonic bath and 160 watt ultrasonic disruptor. A dynamic light scattering technique was used to quantify the volume distribution of the nanoparticles at different sizes after being dispersed by ultrasonic energy. Figure 3.5 shows the volume distribution data for both ultrasonic methods. Both graphs illustrated that the volume distribution of the nanofluids would occur at smaller particle diameters with increasing durations of ultrasonication. However, the difference between 8 and 30 minute time durations for both graphs showed diminishing returns, alluding to approach a critical value correlating with the maximum dispersion possible for each method.

Figure 3.6 shows how the average diameter of the alumina nanoparticles is reduced with increasing specific energy for both methods. The term specific energy was used because, while the sample volume remained constant, the power applied varied. The error bars for Figure 3.6 were quantified using the standard deviation of 10 trials. This study showed a clear agreement with the governing theory. The ultrasonic homogenizer was consistently superior, and because it operated at a higher power output, it could reach its minimum average particle diameter sooner than the bath. This minimum value is roughly at an average diameter of 114 nm corresponding to a specific energy of 8.5 kJ/mL. A specific energy of 8.5 kJ/mL equates to homogenizing a 25 mL nanofluid for 22 minutes at 160 watts. The plateau region for ultrasonic bath started at roughly a specific energy of 7.5 kJ/mL and resulted an average particle diameter of 125 nm. This equates to placing a 25mL nanofluid into a 70 watt ultrasonic bath for 45 minutes.

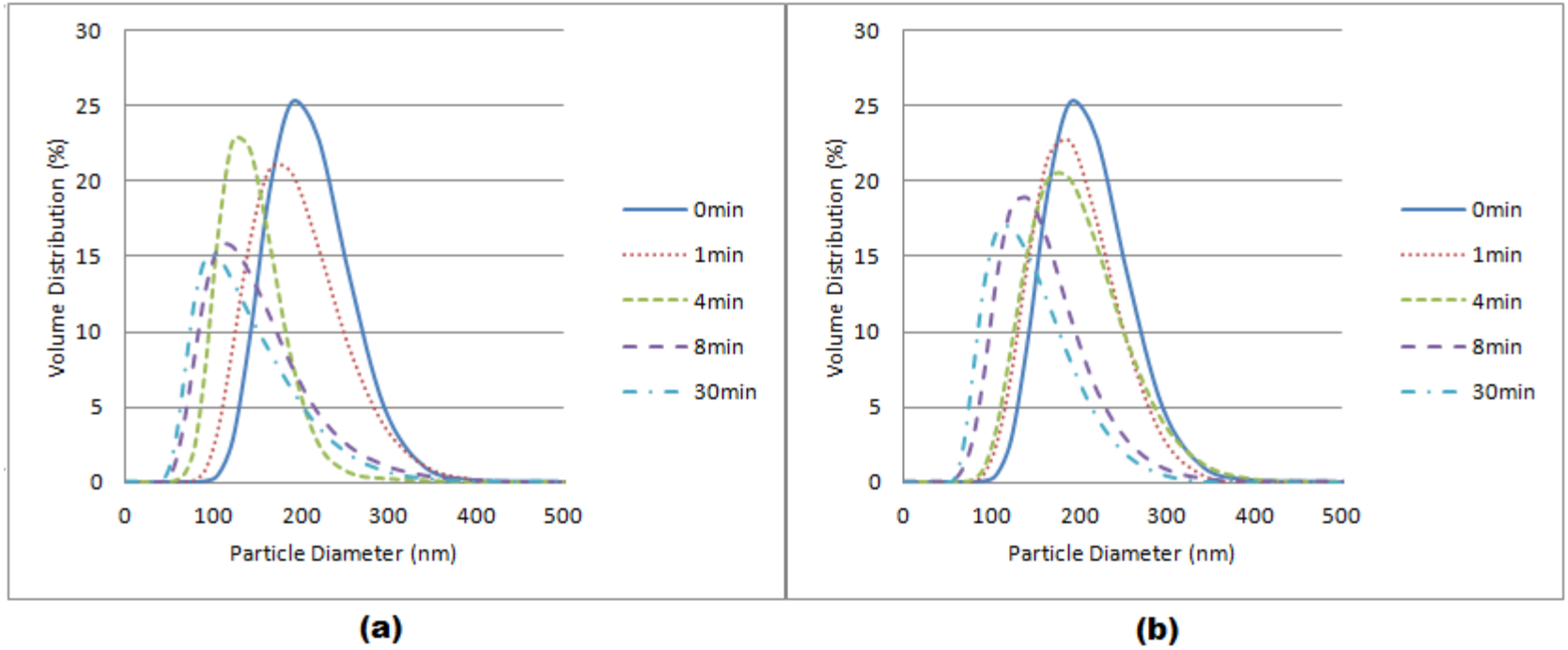

Figure 3.5. Volume Distribution Data against Particle Diameter for (a) 160 Watt Ultrasonic Disruptor and (b) 70 Watt Ultrasonic Bath after Controlled Ultrasonic Time Durations

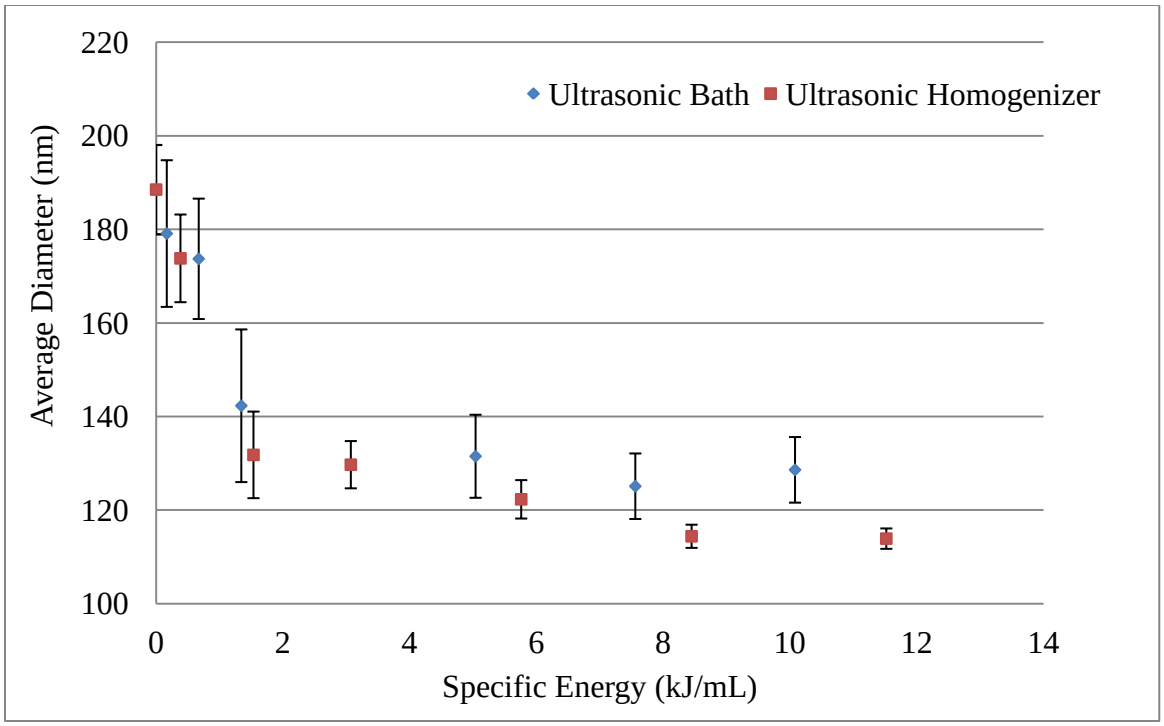

Figure 3.6. Average Particle Size against Specific Energy using Ultrasonic Bath and Ultrasonic Disruptor

3.3 Conclusions

Dry powder analysis was possible through AFM imaging. Contour plots given by this method made it evident that the dry alumina nanopowder was highly agglomerated. Agglomerate sizes ranged upwards of 300 nm with regularity and most nanoclusters were over 150 nm. This agglomerated state was several times that of an ideally monodispersed nanopowder.

An ultrasonic bath and ultrasonic homogenizer were used to investigate the dispersion behavior of alumina nanofluids when applying ultrasonic power. The amount of ultrasonic energy was increased until diminishing returns in average particle size were reached using a dynamic light scattering apparatus. Both dispersion methods showed

marginal benefit of applying additional energy after roughly 8 minutes. When directly compared, ultrasonic homogenization proved to be decisively superior, showing smaller average particle sizes achievable at lower specific energies. The standard deviation of the data using ultrasonic homogenization was also much lower.

CHAPTER FOUR

STABILITY OF NANOFLUIDS

The purpose of this study is to investigate the effect of mixing procedure and surfactant on nanofluid stability. Particle size distribution data was used to determine the best mixing procedure for nanofluids. The stability of nanofluids at different concentrations of nanoparticles and surfactant was visually compared. The stability of nanofluids with two different stabilizing agents was also compared.

Same as described in Chapter 3, the Branson 1510 Ultrasonic Cleaner shown in Figure 3.1 and the ultrasonic homogenizer shown in Figure 3.2 were used for nanofluid mixing and the Malvern Zetasizer Nano ZS was used for particle size distribution analysis.

4.1 Preparation Order for Nanofluids

Preparation order is quite critical for deagglomerating a nanofluid system. The most important step is the time to add the stabilizing agent. If it is added before ultrasonication, heat management issues are significant because oleic acid will degrade at elevated temperatures. However, having the stabilizer present during sonication is beneficial because it will help prevent collisions due to ultrasonication and Brownian motion.

A trial was conducted with two diluted (0.02%wt) alumina nanofluids. With one sample, 0.01 mL of oleic acid was added prior to a 30 minute, 160 watts ultrasonic

homogenization step, while the other after the identical ultrasonication method. Immediately after dispersion, particle sizing analysis was done using the Malvern Zetasizer NS. Figure 4.1 shows the difference between these two scenarios for an alumina nanofluid. A drastic difference in particle size distribution was observed between the two preparation procedures. Having oleic acid present during sonication resulted in some monodispersity, with the maximum agglomerate size at roughly 300 nm. Adding oleic acid immediately after sonication resulted in agglomerates well beyond a micron in size. Thus, adding oleic acid before sonication helped keep particles suspended once deagglomerated and prevented collisions during the ultrasonic process. Therefore, when thermal management was not an issue, this preparation procedure was used when conducting tests.

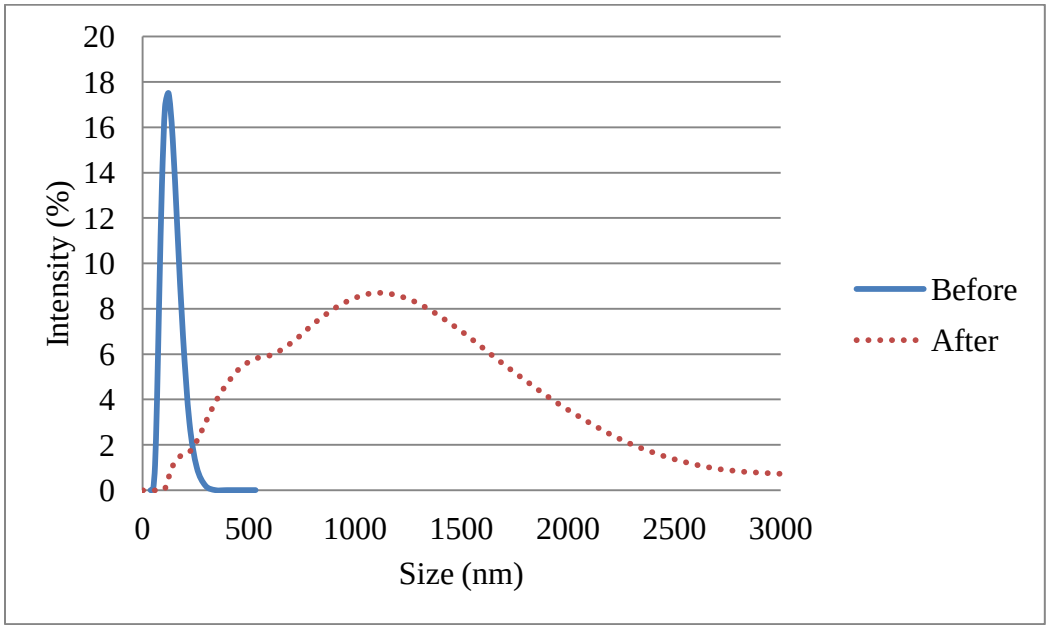

Figure 4.1. Preparation Procedure Study; Adding Oleic Acid Before and After Ultrasonication

4.2 Nanoparticle and Surfactant Concentration on Stability

Effect of the surfactant and nanoparticle concentration on the stability of nanofluids was analyzed by visually examining the sedimentation process over time. Three different alumina concentrations were chosen based on common formulations found in nanofluid literature (2, 1, and 0.5%wt) and were stabilized with three different oleic acid concentrations (14, 9, and 3%wt). Each sample was mixed in accordance to the preparation order study and were all subjected to a 120 watt, 150 second ultrasonic homogenization step.

Figure 4.2 shows the stability at different ratios of oleic acid and nanoparticles after a four day time duration. It is evident that the concentration of oleic acid was critical to creating stable solutions. The most stable of which was a 28:1 ratio between oleic acid and nanoparticles (14%wt Oleic Acid at 0.5%wt Alumina). The sedimentation process over time for this nanofluid was illustrated in Figure 4.3.

4.3 Surfactant Comparison Study

Two samples were made at 31.6 mL P70N oil, 0.276 grams (1.0%wt) alumina nanoparticles, and 0.276 grams (1.0%wt) PIBSA. These samples were then compared to a 1%wt formulation containing ~14%wt oleic acid. Figure 4.4 showed the sample containing oleic acid on the left and the samples containing the PIBSA formulation in the middle and right. After a four day time duration, it was evident that the PIBSA solutions were much more stable. There was no separation at the top and no sedimentation layer at the bottom and only needed 1%wt stabilizer. The oleic acid solution required 14%wt stabilizer and exhibits obvious agglomeration conditions.

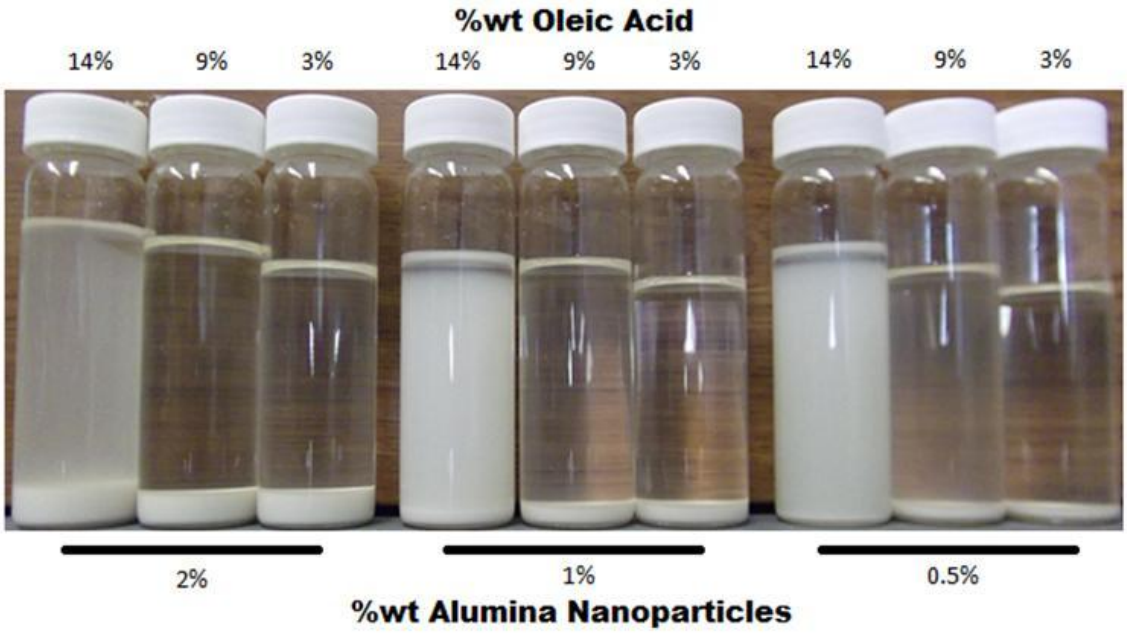

Figure 4.2. Different Sample Concentrations, Four Days after a 120 Watt, 150 Second Disruptor Ultrasonication. *(This figure is presented in color; the black and white reproduction may not be an accurate representation.)*

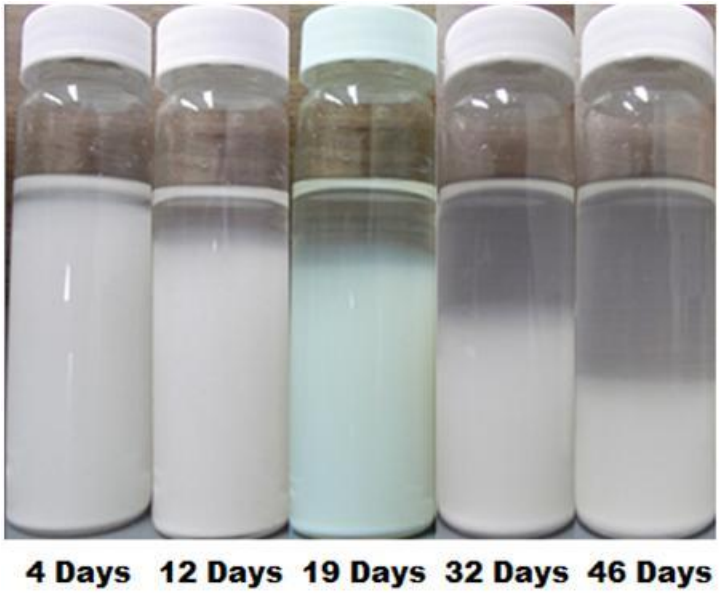

Figure 4.3. 32mL P70N, 14%wt Oleic Acid, 0.5%wt Alumina Nanoparticles Solution over Time. *(This figure is presented in color; the black and white reproduction may not be an accurate representation.)*

Figure 4.4. Oleic Acid Stabilized Nanofluid (Left) vs PIBSA stabilized nanofluids (Middle and Right) after Four Days. *(This figure is presented in color; the black and white reproduction may not be an accurate representation.)*

4.4 Conclusions

A mixing procedure was determined for an alumina nanofluid. Results showed that having the stabilizing agent (oleic acid) present during the application of ultrasonic energy was vital to achieve a well-dispersed nanofluid. This was due to the surfactant preventing collisions between nanoparticles during sonication and the immediate agglomeration once the sonication process was terminated. However, oleic acid was sensitive to heat. A water bath had to be used to manage the heat generated by the ultrasonication process.

Varying nanoparticle and stabilizer concentration was done for an alumina nanofluid using oleic acid as a stabilizing agent to investigate how the ratio affects the stability of the nanofluid. It was concluded that the most stabilizer and the least alumina nanoparticle concentration tested resulted in the most stable nanofluid.

The stabilizing performance of oleic acid was compared against PIBSA. PIBSA showed superior ability to stabilize alumina nanofluids. After a four day time duration, there was no sign of sedimentation or the formation of a supernatant. The concentration necessary to suspend 1%wt alumina nanoparticles was much less than that of oleic acid.

CHAPTER FIVE

TRIBOLOGICAL PERFORMANCE OF NANOFLUIDS

The purpose of this study is to investigate the friction and wear performance of a dispersed and stable alumina nanofluid at two nanoparticle concentrations. Ball-on-disk tests were performed for the nanofluids. The test was repeated using an identical nanofluid with both steel and alumina ceramic balls. Wear area and volume data was collected using an optical surface profiler.

5.1 Experimental Setup

5.1.1 Test Equipment

The Branson 1510 ultrasonic cleaner and the ultrasonic homogenizer were used to mix the nanofluids and the UMT-3 tribometer was used for friction test.

The UMT-3 was equipped with a ball-on-disk test configuration shown in Figure 5.1. An oil circulator was used to take oil from the side of the sample cup and redistribute it to the area of contact. The ball holder prevents the ball from rotating. Therefore, sliding friction is applied, not rolling. A 100 N load sensor was used to provide enough resolution for a low applied load test setup. Coefficient of friction over time data was automatically recorded.

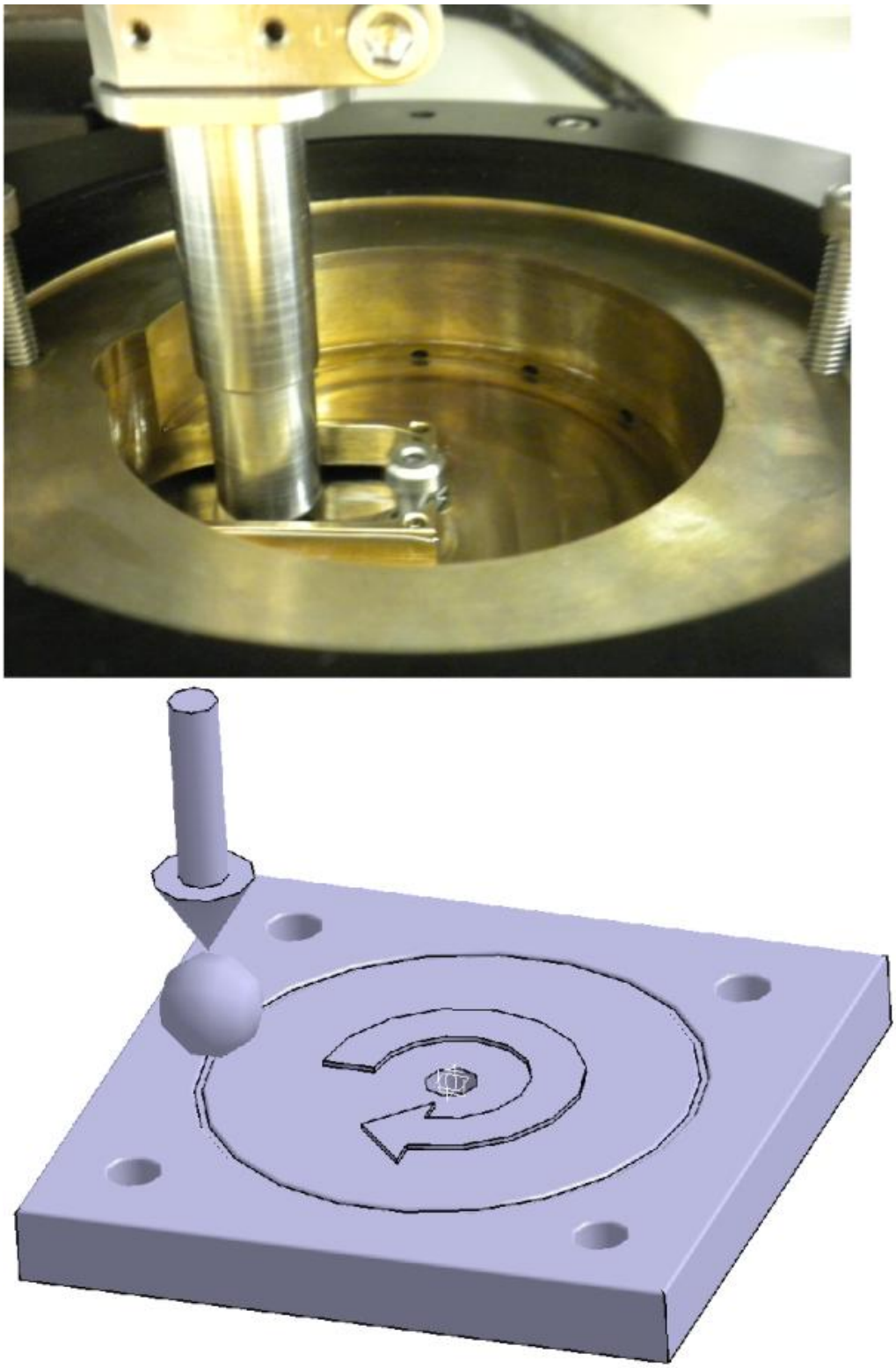

Figure 5.1. UMT-3 Ball-on-Disk Test Setup. *(This figure is presented in color; the black and white reproduction may not be an accurate representation.)*

The resulting wear area and volume from ball-on-disk trials was quantified using the Bruker NPFLEX. The NPFLEX uses vertical scanning interferometry to analyze sub-micron surface contours and sub nano surface roughness properties. Steel disks were measured at eight evenly distributed positions on each wear track to yield a better average. Steel balls were measured once over the full profile of the wear scar. A software package called Vision32 was used for processing the surface profiles.

5.1.2 Sample Preparation

Alumina nanofluids were prepared at 0.5%wt and 2%wt in P70N oil and were stabilized using 14%wt oleic acid. Three controls were also prepared for testing: a neat P70N oil sample, oil with 14%wt oleic acid, and oil with 0.5%wt alumina. The nanofluid samples were first mixed by the ultrasonic bath for 20 minutes. Immediately after, they were additionally dispersed using the ultrasonic homogenizer at 160 watts for 5 minutes. This was done because the ultrasonic bath managed heat more effectively and reduced the average particle size comparable to the ultrasonic homogenizer according to the dispersion study. The ultrasonic homogenizer was used to further disperse the nanofluids beyond the capabilities of the ultrasonic bath.

4140 steel disk samples were polished to a surface roughness of $Ra < 60$ nm with an average roughness of about 30 nm. Five disks were prepared, one for each composition. This was done to prevent possible nanoparticle or surfactant cross-contamination. The hardness of the 4140 steel samples was measured using a Leco R-260 Hardness tester with a 100 kilogram force and a sixteenth inch steel ball indenter. The average HRB hardness measured was 98.7. The experimental hardness

measurements with averages are located as Table A.1 in the appendix. Figure 5.2 shows an example of a polished 4140 steel sample after ball-on-disk tests were conducted. HRC 62, 5/16'', 52100 steel balls were used in a ball-on-disk rotational configuration.

5.2 Results

5.2.1 Steel Ball-on-Disk Tests

Friction tests were conducted for 40-50 nm alumina nanoparticles at 0.5%wt. The oleic acid concentration for nanofluids with stabilizer and the oil with stabilizer control was 14%wt. The applied load was controlled at 4.45 N and the disk with 35 mL of

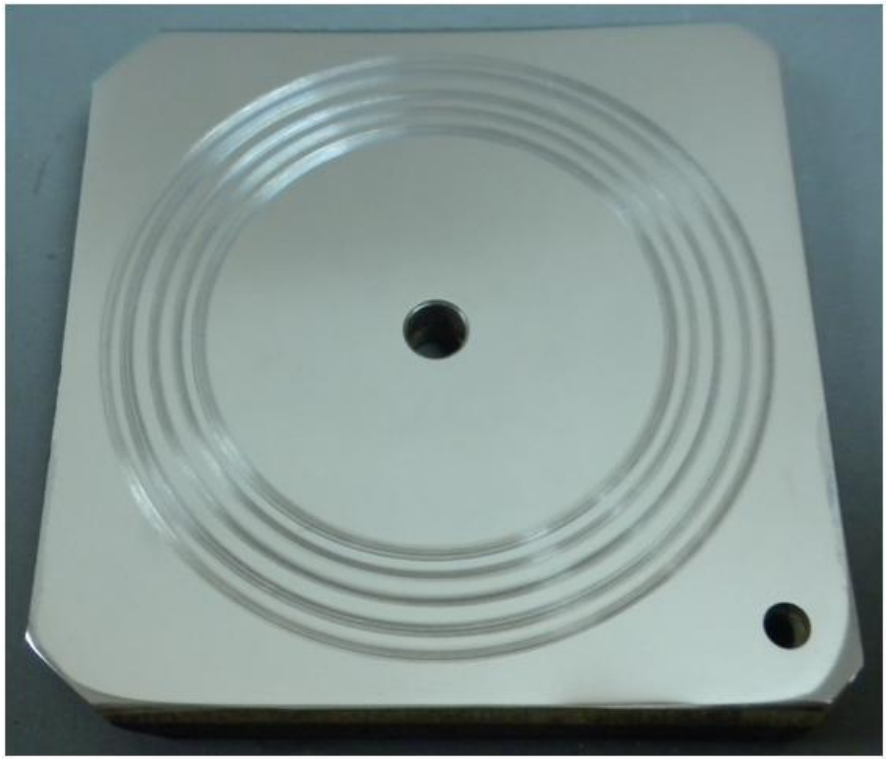

Figure 5.2. Polished 4140 Steel Sample after Ball-on-Disk Trials. *(This figure is presented in color; the black and white reproduction may not be an accurate representation.)*

lubricant rotated at a linear velocity of 1 m/s. Four tests were run with the same nanofluid on the same disk sample at 4 different radii, while the steel ball was replace for each test. The detailed test conditions were shown in Table A.2 in the appendix. Coefficient of friction over time data was acquired and was shown in Figure 5.3. For all cases, the neat P70N oil and oil with surfactant trials were very comparable. The oil with 0.5%wt nanoparticles performed the worst, but the oil with surfactant and nanoparticles did have the lowest coefficient of friction data for the majority of the test. However, all of the stabilized nanofluid trials exhibited a very aggressive run-in period. This very fast decrease in the friction force could allude to a very high abrasive wear rate, which lead to the increasing of the contact area between the two surfaces. This could reduce the contact pressure, thus shift the lubrication regime from mixed lubrication to elastohydrodynamic lubrication. The extremely low coefficient of friction by the end of the trials (~0.03) could also allude to this reasoning. The trials were repeated for a 2%wt alumina nanofluid containing the same amount of oleic acid. The average friction over time data for the four trials for this nanofluid concentration was also shown in Figure 5.3. It was evident that both nanofluid trials showed similar performance. There is a very sharp decrease in the friction force at the start of the test, followed by a constant low friction force. The 2%wt alumina nanofluid trials reached steady conditions slightly sooner and achieved a lower coefficient of friction by the end of the trial. However, this could be due to the lubricant being more abrasive, shifting the lubrication regime from mixed to elastohydrodynamic lubrication sooner because of the higher wear rate at the start of the trials. It is evident that the control samples had no run-in time frame, contrary to both concentrations of alumina nanofluids that were tested.

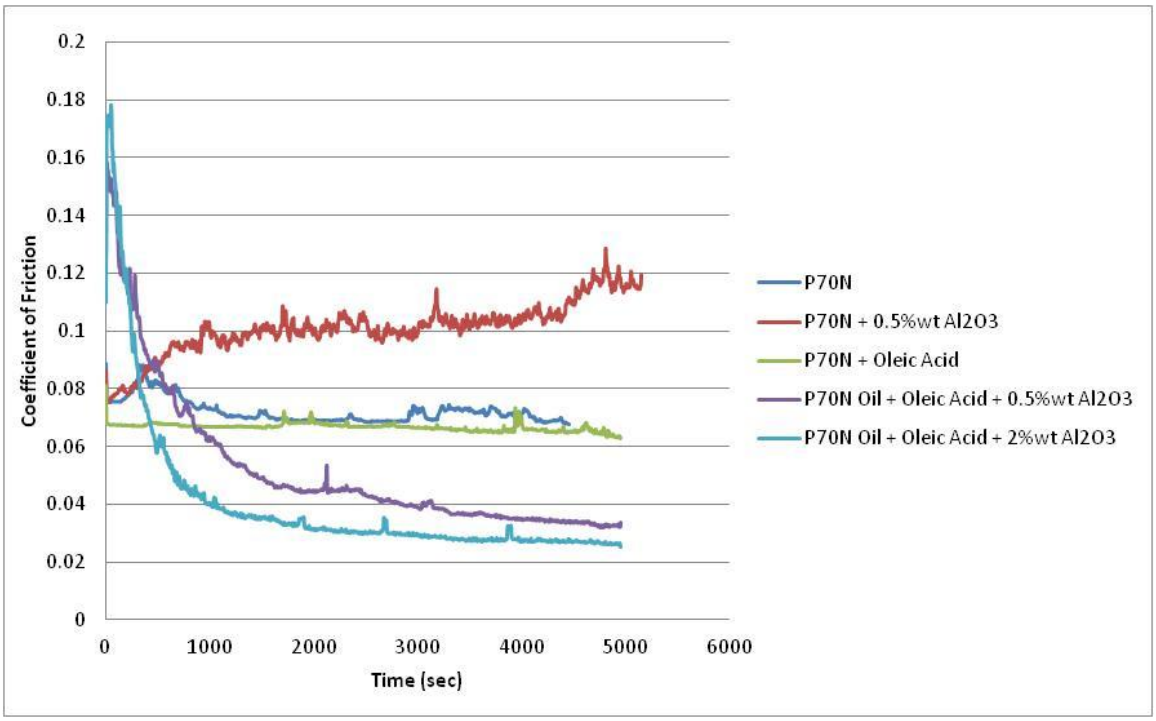

Figure 5.3. Average Coefficient of Friction over Time Data for a 0.5%wt Alumina Nanofluid, 2%wt Alumina Nanofluid, and controls

5.2.2 Steel Ball-on-Disk Wear Data

Wear data was collected using the Bruker NPFLEX to investigate the reason for the aggressive run-in period of the oleic acid stabilized nanofluid trials. Eight positions were chosen on each wear track to get a true average. After analyzing all of the positions, the resulting wear data was found in Figure 5.4 and also shown in Table A.3 in the appendix. The resulting average wear volumes show a 70% increase in wear for the 0.5%wt nanofluid and a 746% increase in wear when the concentration of alumina was increased to 2%wt. This reinforces the run-in assertion at the start of the friction tests.

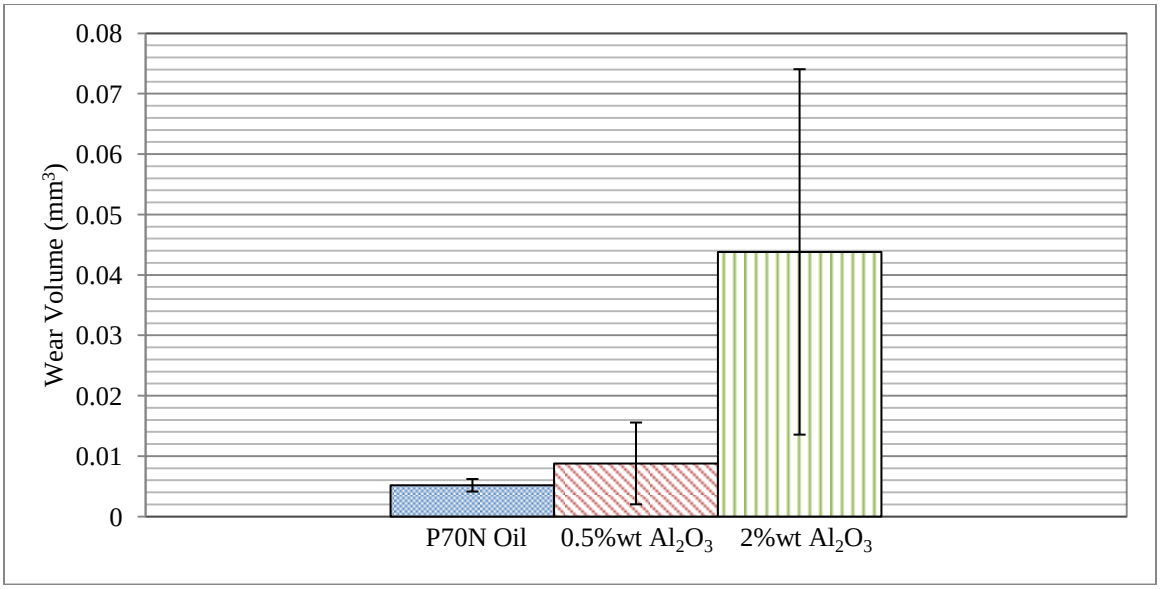

Figure 5.4. Wear track data for the Nanofluids against neat P70N oil

One interesting phenomenon that occurred for all of the nanofluid tests was the appearance of several smaller wear tracks outside of the main track. One example of this was illustrated in Figure 5.5. The left image is a representation of the surface in three-dimensions. The previously polished surface now had separated wear tracks. There was still pristine surface in-between some of these wear tracks. The right image was a typical two-dimensional profile illustrating the severity of the main wear track when compared to neighboring tracks.

Contrary to the nanofluid trials, the wear track profiles for the base fluid were uniform. There was only one wear track and the contour of the wear track was gradual and shallow in comparison. Figure 5.6 shows a typical wear track generated from a ball-on-disk test using the neat base fluid as the lubricant. Outside of the wear track, there are only surface pits that were present from the stock material.

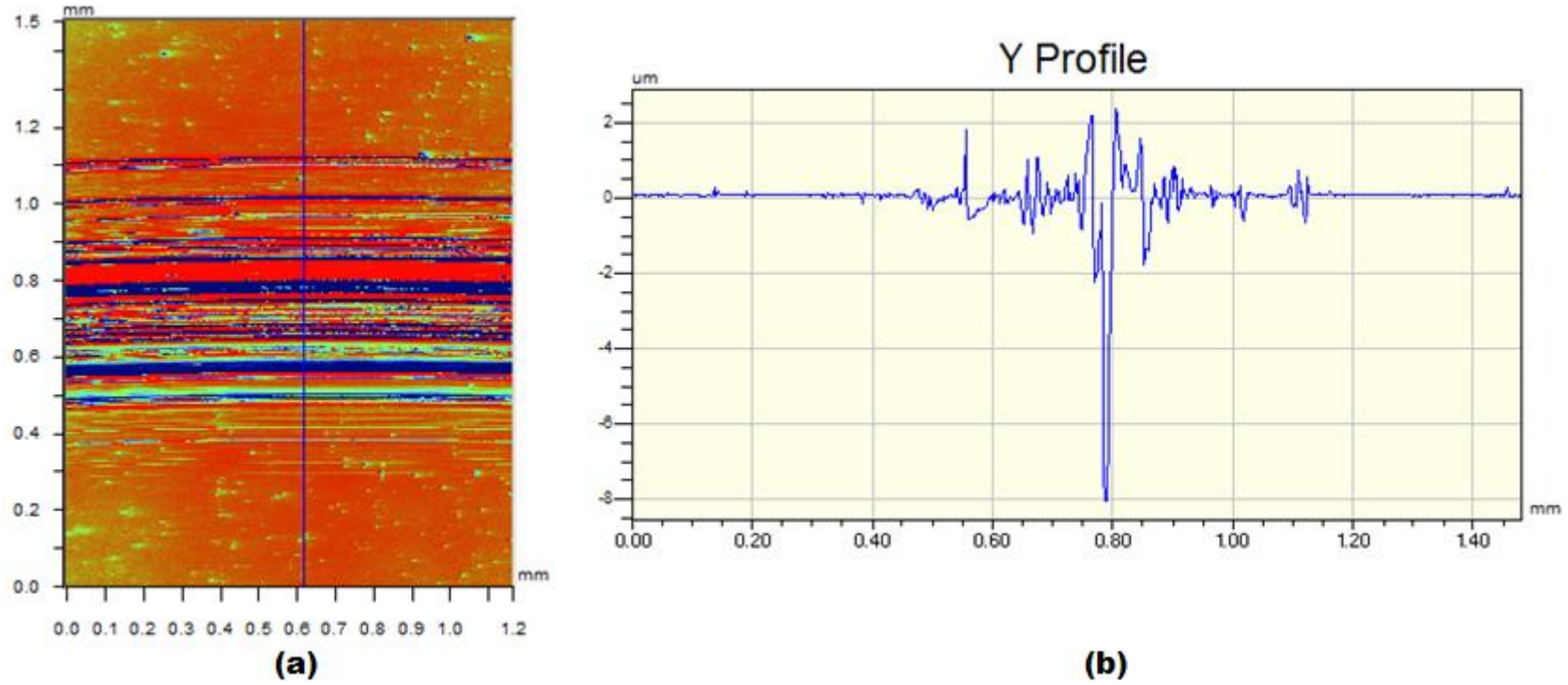

Figure 5.5. NPFLEX contour plots of a 4140 steel wear track after a 0.5%wt nanofluid friction test. *(This figure is presented in color; the black and white reproduction may not be an accurate representation.)*

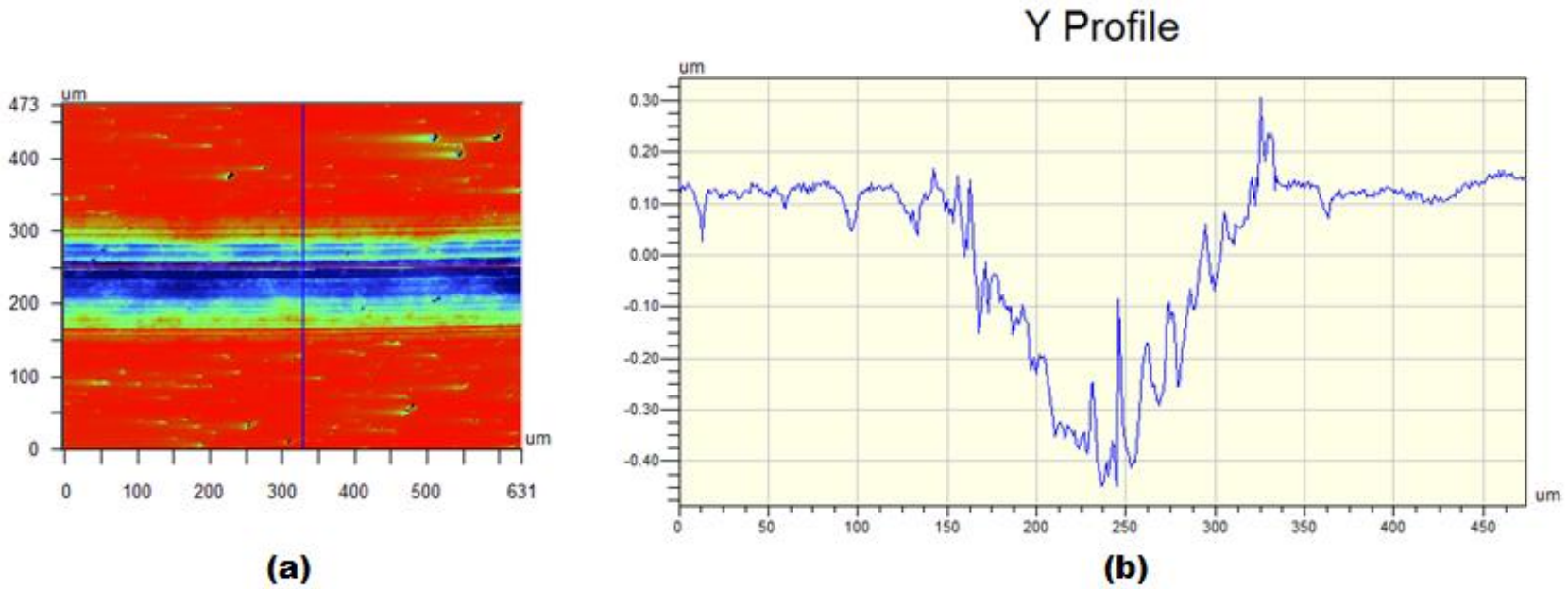

Figure 5.6. NPFLEX contour plots of a 4140 steel wear track after a neat P70N oil friction test. *(This figure is presented in color; the black and white reproduction may not be an accurate representation.)*

To fully understand the occurrence of several wear tracks for the nanofluid trials, the wear scar on the ball was also analyzed. The diameters of the wear scars for the tests were shown in Figure 5.7. Table A.4 in the appendix has the approximate wear volume calculated using the equation for a spherical cap. It was evident that the amount of wear by volume that occurred on the ball was more than three orders of magnitude larger in the nanofluid trials than the oil control. Thus, the alumina caused more abrasive wear on both the 4140 steel and the ball. The amount of wear on the ball was even larger than that of the 4140 steel disk for the nanofluid trials. The wear scar diameter spanned the multiple wear tracks evident on the 4140 steel disk. Even though there was more wear present on both surfaces, because more wear occurred on the bearing steel ball (the harder and more abrasive resistant material) and there was protected surface between the wear tracks of the 4140 steel disk, the alumina nanoparticles showed some potentially beneficial wear performance qualities.

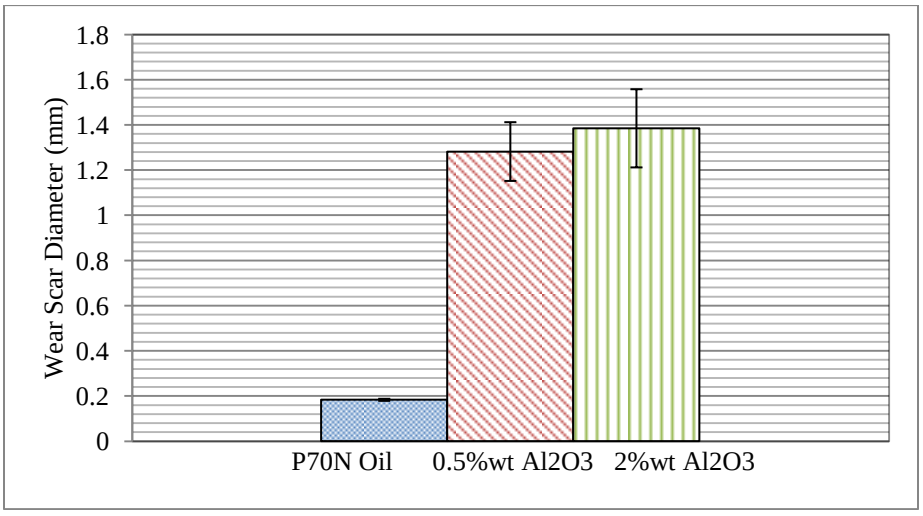

Figure 5.7. Wear scar data for the Nanofluids against neat P70N oil

A specific 0.5%wt nanofluid trial was investigated further to understand the large amounts of wear that were evident on both the 4140 steel disks and 52100 steel balls. A wear profile and the respective wear scar were used for analysis. The three dimensional contour plots generated from the optical surface profiler were used in a comparison shown in Figure 5.8. The aligned three dimensional plots show clear correlation. The peaks of the wear scar directly line up with troughs in the wear track and vice versa. The ball was originally a spherical point contact, but over time turned into a 1.2 mm diameter pin contact. The large amount of area greatly reduced the contact pressure of the constant applied load. There were regions within the wear tracks on 4140 steel profiles where the surface was still of the same starting surface roughness. This effect also reinforced the possibility of alumina nanoparticles embedding into the 4140 steel disk, and protecting it from the harder and more abrasive resistant 52100 bearing steel.

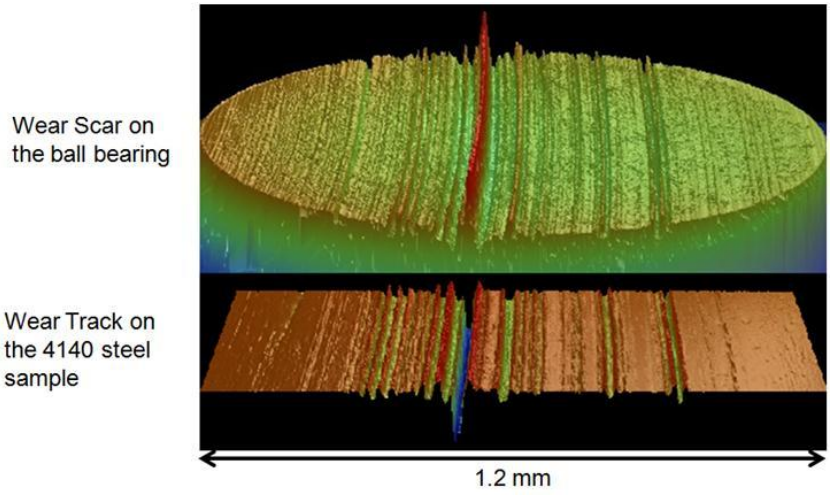

Figure 5.8. Wear Track on 4140 Steel Sample Aligned with Respective Wear Scar on the Ball. *(This figure is presented in color; the black and white reproduction may not be an accurate representation.)*

Scanning electron microscopy (SEM) surpasses the capabilities of visual light based surface profiling techniques. The resolution needed to analyze the effects of nano-sized particles was further investigated using an SEM. After ball-on-disk tests were conducted and wear measurements were taken, a portion of the 4140 steel disk that was used for the 2%wt alumina nanofluid was prepared. A corner of the disk was removed using an abrasive cutter such that a segment of the four wear tracks were represented. The cut sample was then rinsed in acetone and placed in the microscope.

A representative wear track that was created using an alumina nanofluid was selected and investigated for evidence of how the alumina nanoparticles act in an oil lubricant. Although the optical surface profilometer clearly illustrated that the addition of alumina nanoparticles increased wear, the mechanisms remained uncertain.

The same location on a 2% alumina wear track was SEM imaged at four different magnifications: x50, x1,000, x5,000, and x20,000 shown in Figure 5.9. The image taken at x50 magnification (a) shows a wear track spanning over 1 mm in width, which agrees closely to that of the counter-surface wear scar diameters on the 52100 steel balls reported in Table A.4 of the appendix. As the magnification increases, the evidence of finer wear tracks appears all in the same direction of the relative sliding motion. The x20,000 image (d) showed that the width of these small wear tracks ranged from 50 to 200 nm, which was on the same order of the diameter of the alumina nanoparticles(40-50nm). Small scale agglomerates could explain the appearance of larger wear troughs. Due to the emergence of nano-scale toughs in the sliding direction on the 4140 steel surface, it attributed to the ability for alumina nanoparticles to polish the surface. However, there were also neighboring areas with severe abrasive wear.

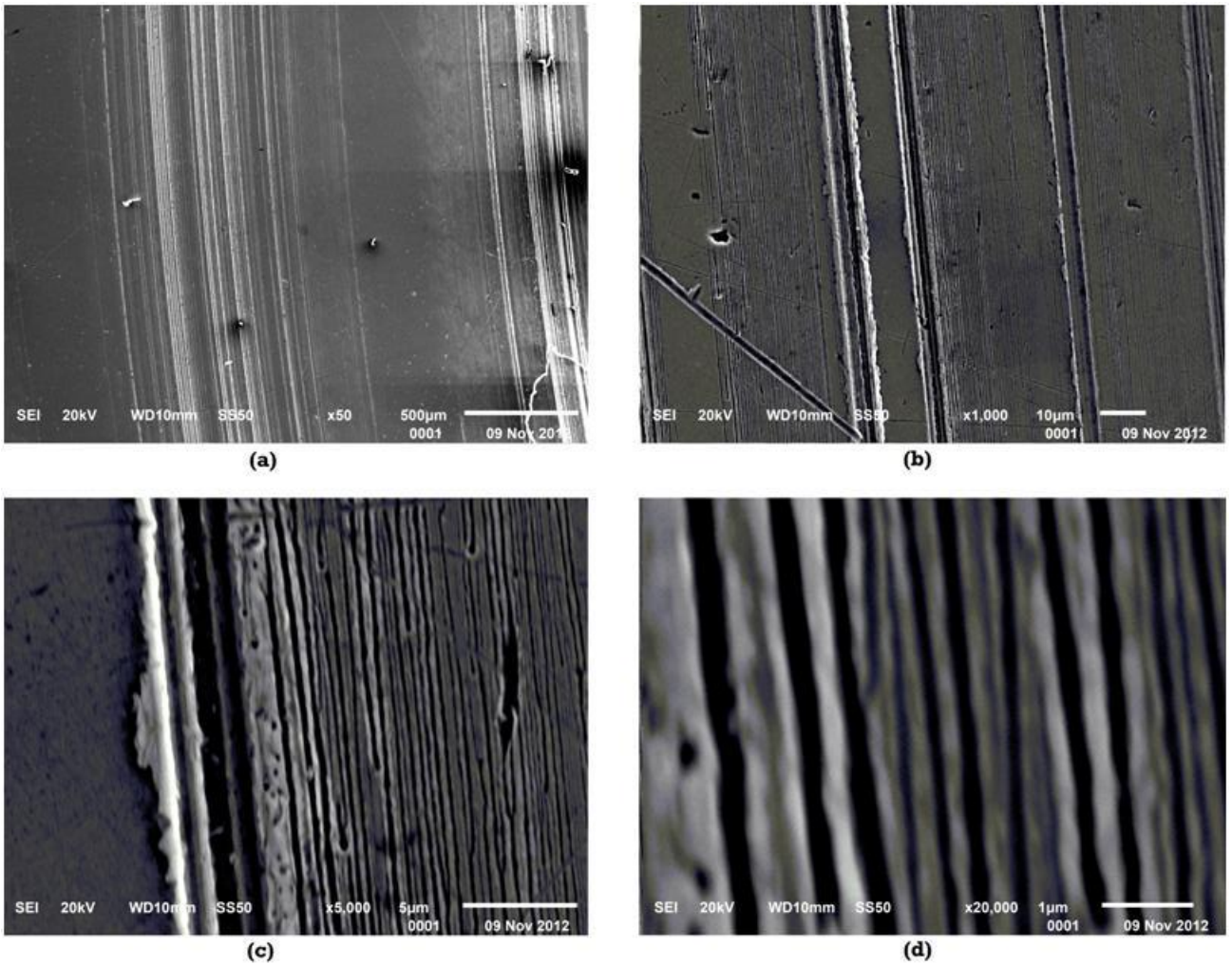

Figure 5.9. SEM images on a 4140 steel sample for a wear track generated by a 2%wt alumina nanofluid at (a) x50, (b) x1000, (c) x5000, and (d) x20,000 magnification.

5.2.3 Ceramic Ball-on-Disk Tests

Due to the severity of the wear scar on the steel ball in the alumina nanofluid trials, a superior abrasive resistant material was chosen. An alumina ceramic ball has the same hardness as the nanoparticles used in the test and was a good candidate to continue investigation because it should have the hardness necessary to prevent major abrasive wear. The same test matrix was run using a 0.5%wt alumina nanofluid, and the resulting friction over time data was shown below in Figure 5.10. There was no run-in at the start of both plots and there was actually a slight reduction of friction at the start of the nanofluid test. This friction reduction decreases over the duration of the test and converged to the control.

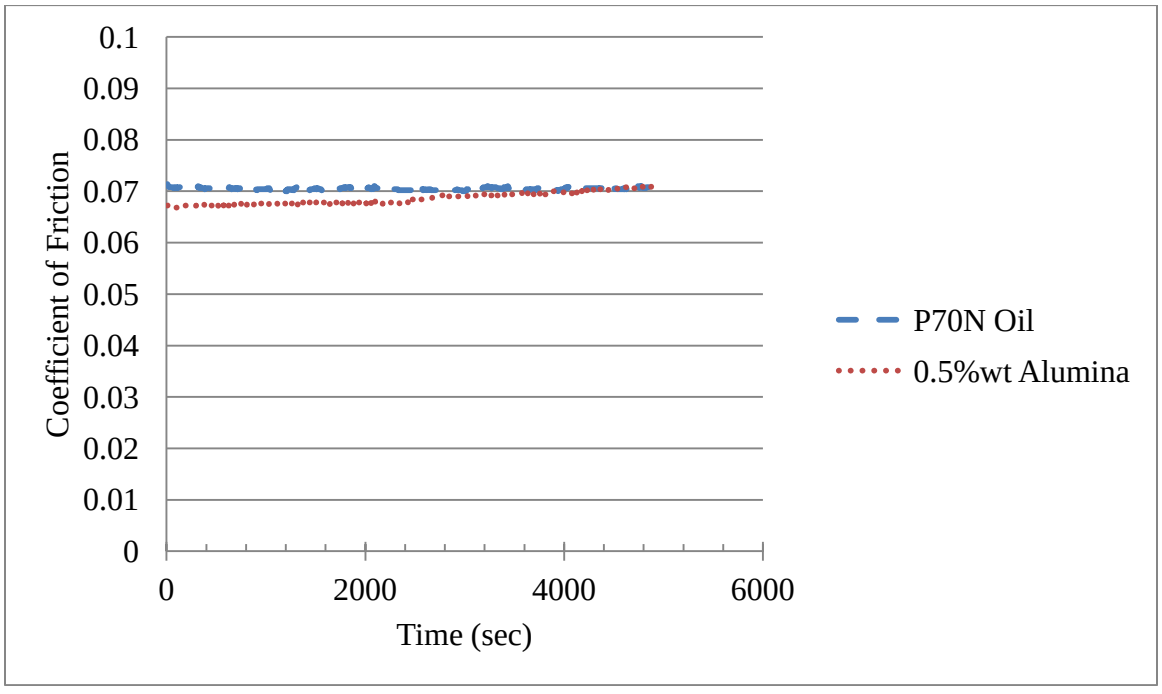

Figure 5.10. Coefficient of friction over time graph for a 0.5%wt alumina nanofluid against neat P70N oil. An average of four trials each.

5.2.4 Ceramic Ball-on-Disk Wear Data

The resulting wear volume data was analyzed for this test and is shown in Figure 5.11. It shows a 53% increase in wear of the 4140 steel disk for the nanofluid trials on average. This is quite similar to the 70% increase in wear for the sample nanofluid formulation when using a bearing steel ball.

The wear tracks for the nanofluid and non-nanofluid trials were quite comparable in geometry even though the nanofluid trials had over fifty perfect more wear. Figures 5.12 and 5.13 showed a typical wear track that resulted from the test matrix. Both two dimensional wear track profiles had only one track, and outside the wear track the steel surface remained the same surface roughness characteristics.

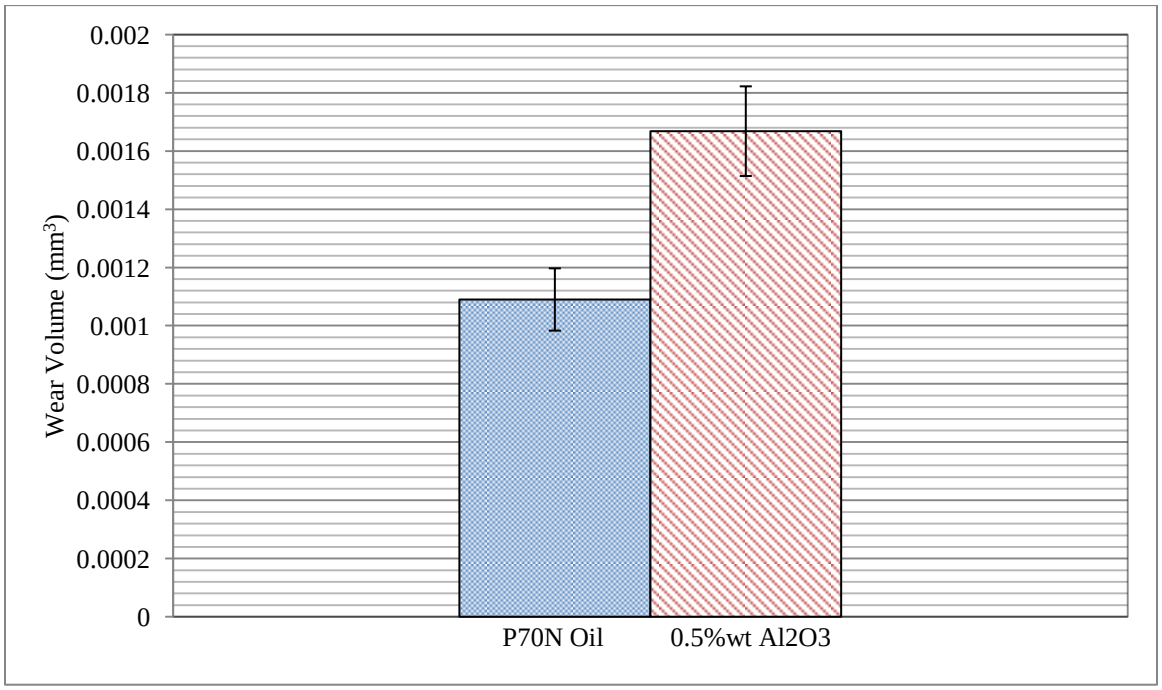

Figure 5.11. Wear track data for the Nanofluids against neat P70N oil

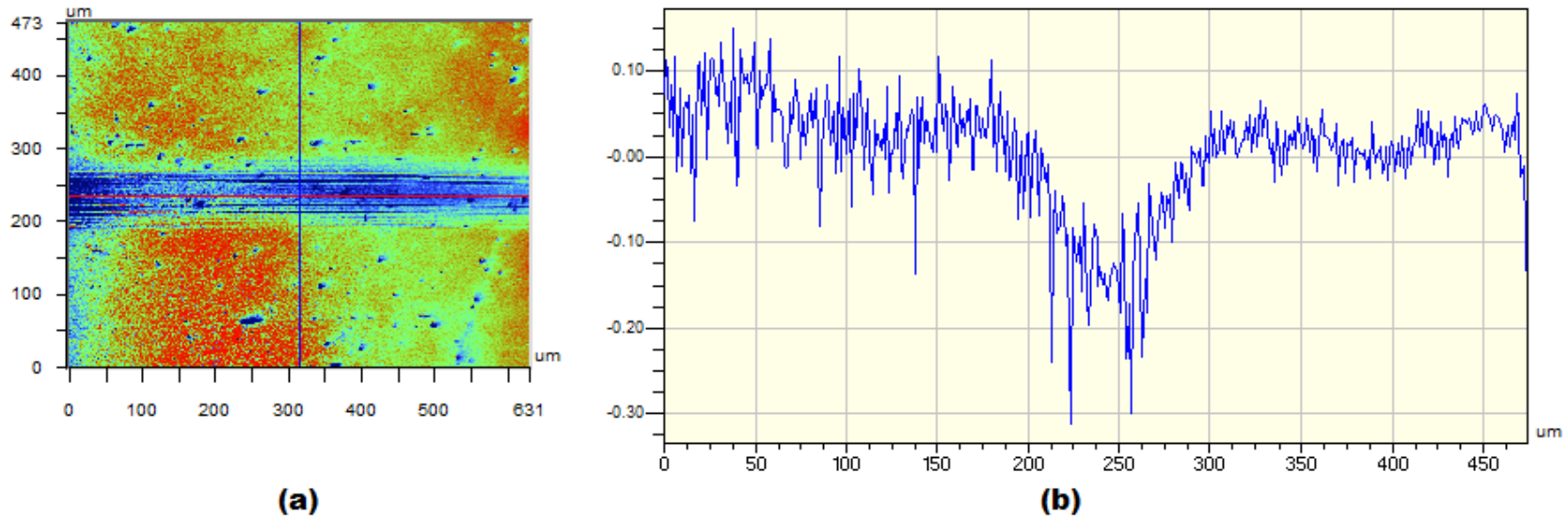

Figure 5.12. NPFLEX contour plots of a 4140 steel wear track after a neat P70N oil friction test using a ceramic ball. *(This figure is presented in color; the black and white reproduction may not be an accurate representation.)*

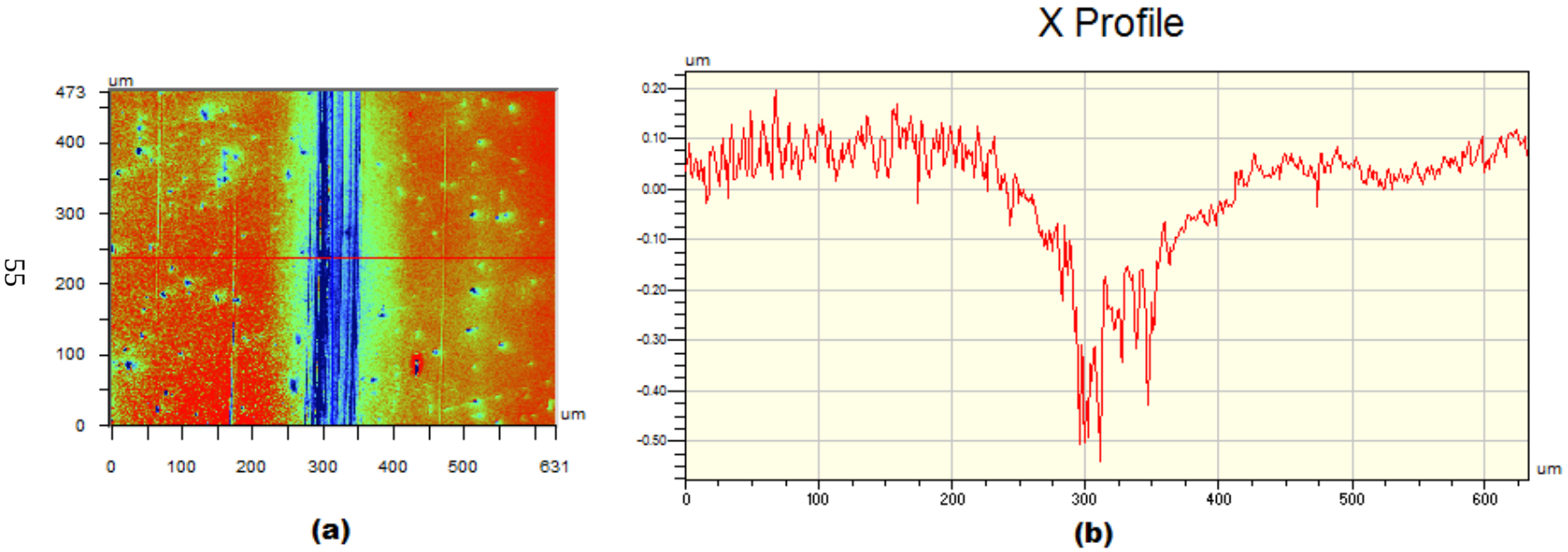

Figure 5.13. NPFLEX contour plots of a 4140 steel wear track after a 0.5%wt Alumina nanofluid friction test using a ceramic ball. *(This figure is presented in color; the black and white reproduction may not be an accurate representation.)*

The wear scar on the alumina ball was not quantifiable with the NPFLEX. There was no evidence of the protection of the 4140 steel using the alumina nanoparticles. This means that the alumina particles primarily acted as third body abrasives in this system rather than providing a layer of embedded particles on the surface. This increased the abrasive wear on the 4140 steel in all tests conducted. A better way to have the particles embed on the surface at the point of contact could prove to reduce the wear and friction of the test.

5.3 Conclusions

The tribological performance of alumina nanofluids was tested using a ball-on-disk configuration in UMT-3 tribometer. A 4140 steel disk was used in conjunction with a 52100 steel ball for the first study. 0.5%wt and 2%wt stabilized alumina nanofluids resulted in a high coefficient of friction at the start of each trial, analogous to that of a large run-in process, alluding to a large amount of wear. The wear scar on the ball and wear track on the disk were analyzed and the alumina nanofluids produced more wear for both concentrations tested. However, there was a larger amount of wear on the more abrasive resistant 52100 steel ball and multiple wear tracks presented on the 4140 steel samples. The wear scar on the ball spanned all of the wear tracks on the 4140 steel, thus there was some protection of the 4140 steel by the alumina nanoparticles as severe wear was occurring on the more abrasive resistant steel ball. The SEM images illustrating nano-width wear tracks present after alumina nanofluid ball-on-disk tests represented the ability for alumina nanoparticles to act as a polishing agent in a working fluid. However, neighboring areas of severe abrasive wear, and the overall increase in wear to both the

4140 steel disk and 52100 steel balls clearly indicated the destructive ability of alumina nanoparticles.

The test was repeated using an alumina ceramic ball to prevent the abrasive wear on the point contact and maintaining the contact pressure more effectively. The resulting ball-on-disk trials showed no run-in process for all trials using a 0.5%wt stabilized alumina nanofluid and a slight reduction in the coefficient of friction (5.5%) at the start of the test. However, this reduction diminished over time until it converged to that of the neat P70N oil control. The resulting wear increase (53%) was similar to that of the steel on steel configuration. The abrasiveness of the alumina nanoparticles was the primary mechanism for all trials due to the large increase in wear.

CHAPTER SIX

THERMAL PROPERTY OF NANOFLUIDS

To investigate the thermal characteristics of an alumina nanofluid, a semi-transient plane method was used to acquire thermal conductivity data. The effect of the stabilizing agent with respect to thermal conductivity was also investigated.

6.1 Experimental Setup

6.1.1 Test Equipment

The Branson 1510 ultrasonic cleaner and the ultrasonic homogenizer were used for nanofluid mixing and the TCi Thermal Conductivity Analyzer was used for thermal property measurement.

The TCi Thermal Conductivity Analyzer employs semi-transient hot plane analysis of solids, powders, and fluids. It can analyze small sample sizes and is not destructive to the test sample. Analysis can be done within a half hour, which is critical when dealing with nanofluid solutions that could potentially be actively agglomerating. This apparatus was used to take thermal conductivity data for four different fluid compositions, i.e. a 1%wt alumina nanofluid containing 14%wt oleic acid in oil, a 1%wt alumina nanofluid without a stabilizing agent in oil, neat oil, and oil containing 14%wt oleic acid only.

6.1.2 Sample Preparation

All fluid samples were first processed in the ultrasonic bath for 20 minutes. Immediately after, they were additionally dispersed using the ultrasonic homogenizer at 160 watts for 5 minutes. Thermal properties were measured after the dispersion process, by extracting 12.5 mL from the center of the sample via a pipette into a cup and engaging the sensor. The thermal conductivity sensor and experimental setup were illustrated in Figure 6.1.

6.2 Results

Four different fluid combinations were tested for thermal properties. The alumina nanoparticles produced a very small amount of thermal conductivity enhancement at 1%wt as shown in Figure 6.2. The percent enhancement by adding 1%wt alumina over neat P70N oil and P70N oil with 14%wt oleic acid was 0.38% and 0.17% respectively.

6.3 Conclusions

The addition of the oleic acid had a larger effect on thermal conductivity enhancement than that of the addition of alumina nanoparticles. The thermal conductivity increase with the addition of alumina was reduced for the stabilized nanofluid. In theory, the more stable, better dispersed nanofluid should exhibit better thermal properties. The reduction in thermal conductivity enhancement could be due to the surfactant coating the nanoparticles, providing an additional barrier for heat to transfer through.

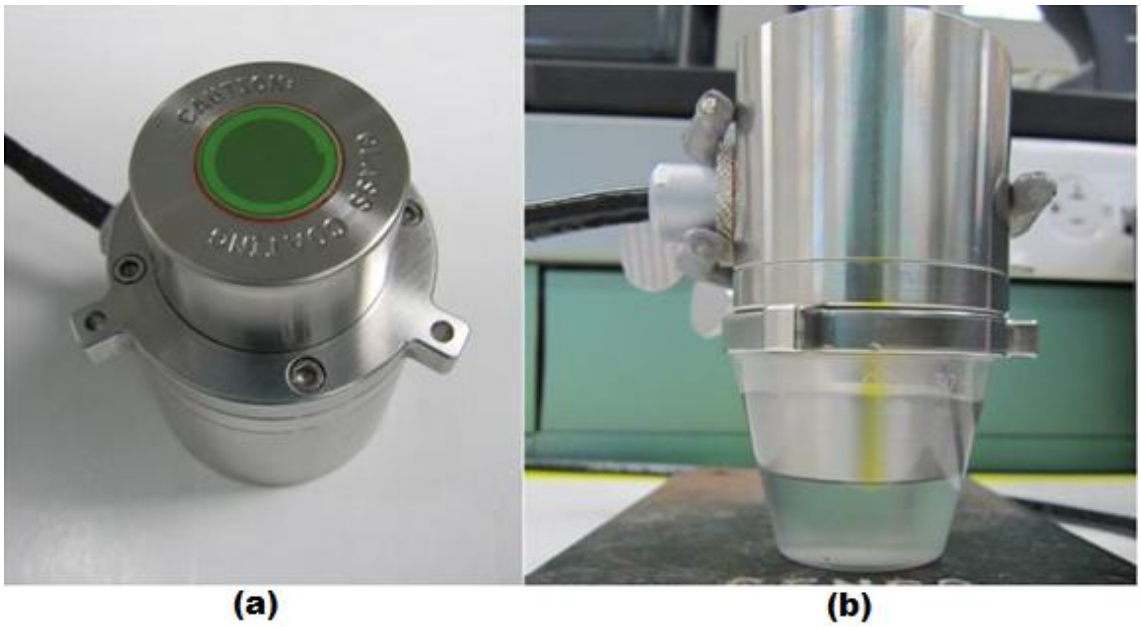

Figure 6.1. TCi Thermal Conductivity Analyzer (Left) and Experimental Setup (Right). *(This figure is presented in color; the black and white reproduction may not be an accurate representation.)*

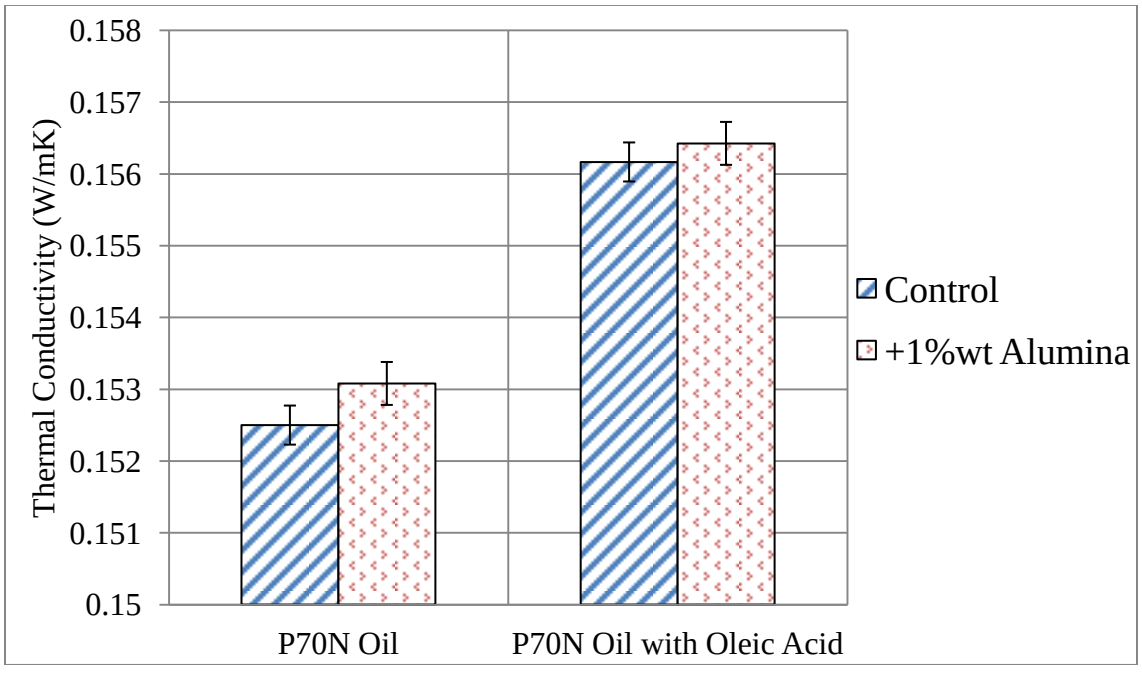

Figure 6.2. Thermal Conductivity Data

CHAPTER SEVEN

CONCLUSIONS

A successful dispersion study was conducted for alumina nanofluids containing oleic acid as a stabilizing agent. This was done with two different ultrasonic dispersing techniques, i.e. ultrasonic bath and ultrasonic homogenizer. Diminishing returns were reached for both methods and the ultrasonic homogenizer achieved smaller average particle sizes at lower energy densities. Therefore, the ultrasonic homogenizer was determined to be the superior dispersing tool for deagglomerating alumina nanofluids.

A mixing procedure for alumina nanofluids was determined. Although oleic acid is sensitive to the heat generated from the ultrasonic homogenization process, it is necessary to prevent particle collisions during dispersion and agglomeration immediately after a dispersion process. If temperature is managed, there should be minimal degradation of the stabilizing agent and produce a superiorly stable, dispersed alumina nanofluid.

Nanoparticle and surfactant concentrations were altered in oil for stability performance. It was determined that the smallest concentration of alumina nanoparticles tested (0.5%wt) paired with the most surfactant (14%wt oleic acid) yielded the most stable solution. This solution was compared to a different stabilizing agent called PIBSA. PIBSA showed no signs of sedimentation or the formation of a supernatant after four days, clearly making it the better stabilizing agent for alumina nanofluids.

Friction tests were performed using alumina nanofluids at two different concentrations. Using a steel ball, the abrasive wear was too high and it resulted in a reduction in contact pressure, shifting the lubrication regime from mixed lubrication to an elastohydrodynamic lubrication regime. However, the presence of pristine surface in-between the multiple wear tracks present on the 4140 steel alluded to particles embedding into the surface and protection from wear in certain areas. SEM images indicated that the alumina nanoparticles acted as polishing additives with the imaging of nano-scale width toughs on the surface of a 4140 steel sample used for a 2%wt alumina nanofluid test. The ball material was changed to an alumina ceramic because of superior abrasion resistance, but the wear tracks on the 4140 steel were still larger. The abrasiveness of the alumina can cause extreme amounts of wear, but if particles are properly embedded on the surface, there is potential for surface protection.

The thermal properties were marginally enhanced using a 1%wt alumina nanofluid. The major increase in thermal conductivity was due to the oleic acid at 14%wt. The percent increase over its respective control was reduced for the stabilized alumina nanofluid, which is contrary to literature [23]. This could be due to a thermal barrier being created by the surfactant coating on the nanoparticles.

Future work on this research would include obtaining x-ray photoelectron spectroscopy data for the wear scars and tracks. This apparatus could help determine the mechanisms in which the alumina nanoparticles acted during ball-on-disk tests. If the hypothesis that some alumina nanoparticles were imbedding into the 4140 steel and protecting the surface from wear was true, there should be increased aluminum concentration in the areas of contact.

Other future work could include applying the dispersion and stability methodology developed to different nanoparticle types. The studies could be augmented to disperse and stabilize pure metals or layered structures (graphite, molybdenum disulfide, tungsten disulfide) in oil. This could greatly ease the process in which to properly test a dispersed and stable nanofluid for tribological and thermal performance.

APPENDIX

DATA TABLES

Table A.1

Experimental 4140 Steel Hardness Measurements. 1/16'' ball, 100 kgf, indentation using a Leco R-260.

	4140 Steel Hardness HRB Trial Number				
Sample	1	2	3	4	Average
1	98.4	98.6	99.2	99.0	98.8
2	97.7	98.5	99.2	98.8	98.6
Overall	---	---	---	---	98.7

Table A.2

Test Conditions for each Ball-on-Disk test of the four trials per fluid tested.

Trial	Radius (mm)	Time (mins)	Speed (rpm)	Speed (m/s)	Rev	Load (lb)
1	16.5	82.5	579	1	477460	1
2	18	90	531	1	477460	1
3	19.5	97.5	490	1	477460	1
4	21	105	455	1	477460	1

Table A.3

Wear volume data for 4140 steel wear tracks.

	Wear Volume (mm^3)		
Trial	P70N Oil	0.5%wt Alumina Nanofluid	2%wt Alumina Nanofluid
1	4.660E-03	1.290E-02	4.608E-02
2	3.968E-03	4.319E-03	2.114E-03
3	6.137E-03	1.608E-02	7.412E-02
4	5.941E-03	1.886E-03	5.294E-02
Average	5.176E-03	8.798E-03	4.381E-02
STDEV	1.039E-03	6.777E-03	3.025E-02

Table A.4

Wear scar data on 52100 Steel ball after ball-on-disk tests. Wear areas are measured experimentally with an optical surface profilometer. Wear volumes are approximated using the equation for the volume of a spherical cap.

	P70N Oil		0.5%wt Alumina Nanofluid		2%wt Alumina Nanofluid	
Trial	Diameter (mm)	Wear Volume (mm^3)	Diameter (mm)	Wear Volume (mm^3)	Diameter (mm)	Wear Volume (mm^3)
1	0.179	1.27E-05	1.172	2.35E-02	1.636	8.99E-02
2	0.180	1.31E-05	1.425	5.16E-02	1.358	4.24E-02
3	0.189	1.59E-05	1.172	2.35E-02	1.276	3.30E-02
4	0.182	1.37E-05	1.358	4.24E-02	1.268	3.23E-02
Average	0.183	1.38E-05	1.282	3.52E-02	1.384	4.94E-02
STDEV	4.56E-03	1.42E-06	1.30E-01	1.41E-02	1.73E-01	2.74E-02

Table A.5

Wear volume data for 4140 steel wear tracks using a ceramic ball.

	Wear Volume (mm^3)	
Trial	P70N Oil	0.5%wt Alumina Nanofluid
1	1.02E-03	1.53E-03
2	1.09E-03	1.78E-03
3	1.00E-03	1.54E-03
4	1.24E-03	1.82E-03
Average	1.09E-03	1.67E-03
STDEV	1.07E-04	1.54E-04

REFERENCES

[1] S. U. S. Choi, "Nanofluids: A new field of scientific research and innovative applications," *Heat Transfer Engineering*, vol. 29, no. 5, pp. 429–431, 2008.

[2] S. U. S. Choi, "Nanofluids: From vision to reality through research," *Journal of Heat Transfer*, vol. 131, no. 3, pp. 1–9, 2009.

[3] J. Buongiorno, D. C. Venerus, N. Prabhat, T. McKrell, J. Townsend, R. Christianson, Y. V. Tolmachev, P. Keblinski, L.-W. Hu, J. L. Alvarado, I. C. Bang, S. W. Bishnoi, M. Bonetti, F. Botz, A. Cecere, Y. Chang, G. Chen, H. Chen, S. J. Chung, M. K. Chyu, S. K. Das, R. Di Paola, Y. Ding, F. Dubois, G. Dzido, J. Eapen, W. Escher, D. Funfschilling, Q. Galand, J. Gao, P. E. Gharagozloo, K. E. Goodson, J. G. Gutierrez, H. Hong, M. Horton, K. S. Hwang, C. S. Iorio, S. P. Jang, A. B. Jarzebski, Y. Jiang, L. Jin, S. Kabelac, A. Kamath, M. A. Kedzierski, L. G. Kieng, C. Kim, J.-H. Kim, S. Kim, S. H. Lee, K. C. Leong, I. Manna, B. Michel, R. Ni, H. E. Patel, J. Philip, D. Poulikakos, C. Reynaud, R. Savino, P. K. Singh, P. Song, T. Sundararajan, E. Timofeeva, T. Tritcak, A. N. Turanov, S. Van Vaerenbergh, D. Wen, S. Witharana, C. Yang, W.-H. Yeh, X.-Z. Zhao, and S.-Q. Zhou, "A benchmark study on the thermal conductivity of nanofluids," *Journal of Applied Physics*, vol. 106, no. 9, 2009.

[4] K. Lee, Y. Hwang, S. Cheong, Y. Choi, L. Kwon, J. Lee, and S. H. Kim, "Understanding the role of nanoparticles in nano-oil lubrication," *Tribology Letters*, vol. 35, no. 2, pp. 127–131, 2009.

[5] S. Stiller, H. Gers-Barlag, M. Lergenmueller, F. Pflucker, J. Schulz, K. P. Wittern, and R. Daniels, "Investigation of the stability in emulsions stabilized with different surface modified titanium dioxides," *Colloids and Surfaces A: Physicochemical and Engineering Aspects*, vol. 232, no. 2–3, pp. 261–267, 2004.

[6] M. J. Mulvihill, S. E. Habas, I. Jen-La Plante, J. Wan, and T. Mokari, "Influence of size, shape, and surface coating on the stability of aqueous suspensions of CdSe nanoparticles," *Chemistry of Materials*, vol. 22, no. 18, pp. 5251–5257, 2010.

[7] S. A. Simakov and Y. Tsur, "Surface stabilization of nano-sized titanium dioxide: Improving the colloidal stability and the sintering morphology," *Journal of Nanoparticle Research*, vol. 9, no. 3, pp. 403–417, 2007.

[8] M. Kole and T. K. Dey, "Viscosity of alumina nanoparticles dispersed in car engine coolant," *Experimental Thermal and Fluid Science*, vol. 34, no. 6, pp. 677–683, 2010.

[9] N. S. Bell, M. E. Schendel, and M. Piech, "Rheological properties of nanopowder alumina coated with adsorbed fatty acids," *Journal of Colloid and Interface Science*, vol. 287, no. 1, pp. 94–106, 2005.

[10] X. Li, D. Zhu, and X. Wang, "Evaluation on dispersion behavior of the aqueous copper nano-suspensions," *Journal of Colloid and Interface Science*, vol. 310, no. 2, pp. 456–463, 2007.

[11] R. Somasundaran and L. Huang, "Adsorption Behavior of Surfactant Mixtures at Solid-Liquid Interface," *Polish Journal of Chemistry*, vol. 71, no. 5, pp. 568–568, 1997.

[12] E. Amstad, S. Zurcher, A. Mashaghi, J. Y. Wong, M. Textor, and E. Reimhult, "Surface functionalization of single superparamagnetic iron oxide nanoparticles for targeted Magnetic resonance imaging," *Small*, vol. 5, no. 11, pp. 1334–1342, 2009.

[13] F. Chemat, I. Grondin, P. Costes, L. Moutoussamy, A. S. C. Sing, and J. Smadja, "High power ultrasound effects on lipid oxidation of refined sunflower oil," *Ultrasonics Sonochemistry*, vol. 11, no. 5, pp. 281–285, 2004.

[14] P. Ding and A. W. Pacek, "Ultrasonic processing of suspensions of hematite nanopowder stabilized with sodium polyacrylate," *AIChE Journal*, vol. 55, no. 11, pp. 2796–2806, 2009.

[15] J. Xiong, S. Xiong, Z. Guo, M. Yang, J. Chen, and H. Fan, "Ultrasonic dispersion of nano TiC powders aided by Tween 80 addition," *Ceramics International*, vol. 38, no. 3, pp. 1815–1821, 2012.

[16] P. Bihari, M. Vippola, S. Schultes, M. Praetner, A. G. Khandoga, C. A. Reichel, C. Coester, T. Tuomi, M. Rehberg, and F. Krombach, "Optimized dispersion of nanoparticles for biological in vitro and in vivo studies," *Particle and Fibre Toxicology*, vol. 5, Nov. 2008.

[17] Y. Hwang, J.-K. Lee, J.-K. Lee, Y.-M. Jeong, S. Cheong, Y.-C. Ahn, and S. H. Kim, "Production and dispersion stability of nanoparticles in nanofluids," *Powder Technology*, vol. 186, no. 2, pp. 145–153, 2008.

[18] G. Roebben, S. Ramirez-Garcia, V. A. Hackley, M. Roesslein, F. Klaessig, V. Kestens, I. Lynch, C. M. Garner, A. Rawle, A. Elder, V. L. Colvin, W. Kreyling, H. F. Krug, Z. A. Lewicka, S. McNeil, A. Nel, A. Patri, P. Wick, M. Wiesner, T. Xia, G. Oberdorster, and K. A. Dawson, "Interlaboratory comparison of size and surface charge measurements on nanoparticles prior to biological impact assessment," *Journal of Nanoparticle Research*, vol. 13, no. 7, pp. 2675–2687, 2011.

[19] D. Zhu, X. Li, N. Wang, X. Wang, J. Gao, and H. Li, "Dispersion behavior and thermal conductivity characteristics of Al2O3-H2O nanofluids," *Current Applied Physics*, vol. 9, no. 1, pp. 131–139, 2009.

[20] H. T. Zhu, C. Y. Zhang, Y. M. Tang, and J. X. Wang, "Novel synthesis and thermal conductivity of CuO nanofluid," *Journal of Physical Chemistry C*, vol. 111, no. 4, pp. 1646–1650, 2007.

[21] Y. Xuan and Q. Li, "Heat transfer enhancement of nanofluids," *Kung Cheng Je Wu Li Hsueh Pao/Journal of Engineering Thermophysics*, vol. 21, no. 4, pp. 466–470, 2000.

[22] J. A. Eastman, U. S. Choi, S. Li, L. J. Thompson, and S. Lee, "Enhanced thermal conductivity through the development of nanofluids," in *Proceedings of the 1996 MRS Fall Symposium, December 2, 1996 - December 5, 1996*, 1997, vol. 457, pp. 3–11.

[23] A. Nasiri, M. Shariaty-Niasar, A. Rashidi, A. Amrollahi, and R. Khodafarin, "Effect of dispersion method on thermal conductivity and stability of nanofluid," *Experimental Thermal and Fluid Science*, vol. 35, no. 4, pp. 717–723, 2011.

[24] A. Hernandez Battez, R. Gonzalez, J. L. Viesca, J. E. Fernandez, J. M. Diaz Fernandez, A. Machado, R. Chou, and J. Riba, "CuO, ZrO2 and ZnO nanoparticles as antiwear additive in oil lubricants," *Wear*, vol. 265, no. 3–4, pp. 422–428, 2008.

[25] L. Gara and Q. Zou, "Friction and Wear Characteristics of Water-Based ZnO and Al2O3 Nanofluids," *Tribology Transactions*, vol. 55, no. 3, pp. 345–350, 2012.

[26] C. GU, Q. LI, Z. GU, and G. ZHU, "Study on application of CeO2 and CaCO3 nanoparticles in lubricating oils," *Journal of Rare Earths*, vol. 26, no. 2, pp. 163–167, 2008.

[27] C. Gu, G. Zhu, L. Li, X. Tian, and G. Zhu, "Tribological effects of oxide based nanoparticles in lubricating oils," *Journal of Marine Science and Application*, vol. 8, no. 1, pp. 71–76, Mar. 2009.

[28] H. YU, Y. XU, P. SHI, B. XU, X. WANG, and Q. LIU, "Tribological properties and lubricating mechanisms of Cu nanoparticles in lubricant," *Transactions of Nonferrous Metals Society of China (English Edition)*, vol. 18, no. 3, pp. 636–641, 2008.

[29] X. L. Wang, B. S. Xu, Y. Xu, H. L. Yu, P. J. Shi, and Q. Liu, "Preparation of nano-copper as lubrication oil additive," *Journal of Central South University of Technology*, vol. 12, pp. 203–206, Oct. 2005.

[30] Z. S. Hu, R. Lai, F. Lou, L. G. Wang, Z. L. Chen, G. X. Chen, and J. X. Dong, "Preparation and tribological properties of nanometer magnesium borate as lubricating oil additive," *Wear*, vol. 252, no. 5–6, pp. 370–374, 2002.

[31] J. F. Zhou, Z. S. Wu, Z. J. Zhang, W. M. Liu, and Q. J. Xue, "Tribological behavior and lubricating mechanism of Cu nanoparticles in oil," *Tribology Letters*, vol. 8, no. 4, pp. 213–218, 2000.

[32] A. Moshkovith, V. Perfiliev, A. Verdyan, I. Lapsker, R. Popovitz-Biro, R. Tenne, and L. Rapoport, "Sedimentation of IF-WS2 aggregates and a reproducibility of the tribological data," *Tribology International*, vol. 40, no. 1, pp. 117–124, 2007.